

Convolutional Autoencoder for Studying Dynamic Functional Brain Connectivity in Resting-State Functional MRI

Fatemeh Mohammadi

A Thesis

In the Department

of

Electrical and Computer Engineering

Presented in Partial Fulfillment of the Requirements for the Degree of

Master of Science (Electrical and Computer Engineering) at

Concordia University

Montreal, Quebec, Canada

April 2019

© Fatemeh Mohammadi, 2019

CONCORDIA UNIVERSITY
School of Graduate Studies

This is to certify that the thesis prepared

By: **Fatemeh Mohammadi**

Entitled: **Convolutional Autoencoder for Studying Dynamic Functional Brain
Connectivity in Resting-State Functional MRI**

and submitted in partial fulfillment of the requirements for the degree of

Master of Applied Science (Electrical and Computer Engineering)

Complies with the regulations of the University and meets the accepted standards with respect to originality and quality.

Signed by the final examining committee:

_____ Chair
Dr.

_____ External Examiner
Dr.

_____ Examiner
Dr.

_____ Supervisor
Dr. M. O. Ahmad

_____ Supervisor
Dr. M.N.S. Swamy

Approved by _____
Dr. W. E. Lynch, Chair Department of
Electrical and Computer Engineering

_____2019 _____
Dr. Amir Asif, Dean
Faculty of Engineering and Computer Science

ABSTRACT

Convolutional Autoencoder for Studying Dynamic Functional Brain Connectivity in Resting-State Functional MRI

Fatemeh Mohammadi

Brain is the most complex organ in human body. Understanding how different regions of the brain function and interact with one another is a challenging task. One of the most important topics in the study of the brain is the functional brain connectivity, which is defined as the correlations, each between a pair of the activation signals from the different regions of the brain. Study of the functional connectivity in the human brain provides new insights into the understanding of the healthy and diseased brains and their differences. Functional magnetic resonance imaging (fMRI) is an imaging technique that allows researchers to study the brain activity and functional connectivity. While many researchers have focused on static functional connectivity in the resting-state fMRI to study the functions of the brain, dynamic functional connectivity has received more attention recently for such a study, since it provides more detailed information about the brain functions. Within the literature for studying the dynamic brain connectivity, k-means clustering has been applied to the connectivity matrices in order to find the functional connectivity patterns. However, it is known that the k-means clustering technique is not suitable for applying it to high dimensional data such as the functional brain connectivity matrices. In this thesis, in order to overcome this problem, we propose a deep learning-based convolutional autoencoder to obtain

latent representations of the connectivity matrices prior to applying to them the k-means clustering. Use of the convolutional autoencoder, not only reduces the dimension of the connectivity matrices, but also provides a more semantic representation of these matrices. It is shown that the proposed method of clustering that consists of the use of the autoencoder followed by k-means clustering results in improving the clustering of the connectivity matrices, and consequently, to a better capturing of the functional connectivity patterns. In order to show the effectiveness of the proposed clustering method, synthetic connectivity matrices for patterns, with their classes known, are generated. The proposed method is then first applied to these syntactically generated connectivity matrices and the resulting patterns are compared with that obtained by applying k-means clustering technique to the synthetic connectivity matrices. It is shown that the proposed method classifies the various patterns more accurately.

The proposed method is then used to study the dynamic functional brain connectivity by applying it to real fMRI data captured from a group of healthy subjects and another group of subjects affected by schizophrenia. For this purpose, after preprocessing the raw fMRI data for each subject in these two groups, the group independent component analysis (ICA) is applied in order to decompose the fMRI data into statistically independent components (map of the entire brain) and their corresponding time-courses. Each independent component corresponds to a specific region of the brain. The connectivity matrix whose elements corresponds to the correlation between the time-courses within a segment of the time-courses enclosed inside a sliding window is then obtained. Next, the proposed clustering method is used to cluster all the connectivity matrices, each corresponding to one segment, into a finite number of functional connectivity patterns (states). A two-sample t-test is then performed on each state in order to determine each pair of the regions in the group of the healthy control subjects for which weather or not the correlation value

is significantly different from that of the corresponding pair of the regions in the group of schizophrenia patients. It is observed through this test that there are indeed pairs of the brain regions where significant differences do exist between the two groups. It is also seen that such a difference between the two groups is even more pronounced in the visual network of the brain.

Finally, in this thesis, a study is undertaken for the evaluation of the dwell time, which is defined to be the duration for a functional connectivity pattern to remain in one state before switching to another state. It is shown through this study that the dwell time for the healthy group to stay in the state with more connectivity is longer than that for the group with schizophrenia. On the other hand, the dwell time for the group with schizophrenia to stay in the state with less connectivity is longer than that for the healthy group.

ACKNOWLEDGEMENTS

It is my pleasure to express my deep gratitude and thanks to my supervisors, Professor M.O. Ahmad and Professor M.N.S Swamy for their continuous guidance and support throughout the course of this research. Their valuable suggestions have been very useful and were among the major reasons that enabled me to pursue my research. It has been an honor and privilege to work under their supervision. I would never forget their support and affection throughout my research period, and I am deeply grateful for them.

Special thanks and gratitude are due to my beloved husband, Yaser, for his patience, encouragement and support. I am so thankful to have him in my life. I would like also to thank my parents and friends who supported me and were available in times of need and eased the hardships of my life. Special gratitude to my mother and my father who are the first inspiration for me in the field of research work.

TABLE OF CONTENTS

LIST OF FIGURES	X
LIST OF TABLES	XIV
LIST OF SYMBOLS	XV
LIST OF ABBRIVIATIONS	XVII
CHAPTER 1: Introduction.....	1
1.1 Background	1
1.2 Human Brain.....	1
1.3 Functional and Anatomical Brain Connectivity	2
1.4 Functional MRI.....	3
1.5 Resting-State fMRI	5
1.6 Resting-State Networks	7
1.7 Static and Dynamic Functional Connectivity	7
1.8 Functional Connectivity Analysis	8
1.9 Brief Literature Review Survey	9
1.10 Motivation and Thesis Objective	10
1.11 Organization of the Thesis	11
CHAPTER 2: Background Material.....	13
2.1 Introduction.....	13
2.2 Preprocessing of fMRI Images	13
2.2.1 Slice Timing Correction.....	13
2.2.2 Realignment	14

2.2.3 Coregistration.....	15
2.2.4 Normalization	16
2.2.5 Spatial Smoothing.....	16
2.3 Independent Component Analysis	17
2.4 ICA in fMRI.....	19
2.5 Group ICA	21
2.6 Component Selection.....	23
2.7 Dynamic Functional Brain Connectivity	25
2.8 K-means Technique	27
2.9 Two-Sample T-Test	29
2.10 Summary	30
CHAPTER 3: Group Difference Study Using Convolutional Autoencoder.....	31
3.1 Introduction.....	31
3.2 Introduction to Neural Networks	32
3.3 Convolutional Neural Networks	35
3.3.1 Convolutional Layer	36
3.3.2 Pooling Layer.....	38
3.4 Convolutional Autoencoder.....	39
3.5 The Pipeline of Dynamic Functional Brain Connectivity Study	41
3.5.1 Group ICA and Windowing.....	41
3.5.2 Convolutional Autoencoder for Obtaining FC States.....	41
3.5.3 Group Analysis Study	43

3.6 Summary	43
CHAPTER 4: Results and Discussions	45
4.1 Introduction.....	45
4.2 What Is Schizophrenia?	46
4.3 fMRI Data Analysis	46
4.4 Analysis of Group Differences	62
4.5 Summary	68
CHAPTER 5: Conclusion and Future Work	70
5.1 Conclusion	70
5.2 Future Work	72
REFERENCES	73

List of Figures

Figure 1.1:	a) The structure of a typical neuron in human brain [3].	
	b) A vertical cut of brain showing grey matter and white matter tissues [4]	2
Figure 1.2:	a) White matter fiber tracking using DTI.	
	b) Functional connectivity map showing the coactivation between some brain regions [7].....	3
Figure 1.3:	Increasement in blood flow resulted from brain neural activity leads to increasing glucose and oxygen and decreasing in deoxyhemoglobin [17]	4
Figure 1.4:	fMRI data as a time sequence of 3D images [18].....	5
Figure 1.5:	An fMRI scanner; a functional magnetic resonance imaging equipment using a strong magnetic field to measure brain activity [24].....	6
Figure 1.6:	Common resting-state networks [25]	7
Figure 2.1:	Time slicing, a preprocessing step for fMRI data [42,43].....	14
Figure 2.2:	Realignment of slices.....	15
Figure 2.3:	Coregistration, aligning the functional MRI data with structural image.....	15
Figure 2.4:	MNI space, averaged anatomical images of 152 subjects [45].....	16
Figure 2.5:	Separating mixed speech data recorded by microphones using ICA [47]	17
Figure 2.6:	Applying ICA to fMRI data.....	18

Figure 2.7:	Decomposition of fMRI images using ICA. Each row of X is a scan of brain flattened at a certain time point; Each column of A is a coefficient (time course) of the corresponding component; Each row of S is an independent component [50]	20
Figure 2.8:	Applying ICA to the concatenated dimension reduced data of different subjects	21
Figure 2.9:	An example of the brain functional connectivity matrix. The independent brain components are separated into seven groups. Sub-cortical (SC), auditory (AUD), visual (VIS), sensorimotor (SM), cognitive control (CC), default mode (DM) and cerebellar (CB)	25
Figure 2.10:	Obtaining the functional connectivity matrices by using a sliding window [52]	27
Figure 2.11:	K-means clustering fails to put image (b), (c) and (d) in the same cluster as image (a) [54]	28
Figure 2.12:	Two independent populations [55]	29
Figure 3.1:	The pipeline of dynamic functional brain connectivity study	31
Figure 3.2:	The physiological representation of a neuron [57]	32
Figure 3.3:	The computation in a neuron	33
Figure 3.4:	The most common activation functions [59]	33
Figure 3.5:	A typical structure of a multi-layer neural network.....	35
Figure 3.6:	A typical architecture of a convolutional neural network [60].....	36
Figure 3.7:	An example of zero padding operation.....	37

Figure 3.8:	Max pooling operation [63].....	38
Figure 3.9:	The general architecture of a convolutional autoencoder [64].....	40
Figure 4.1:	An independent component (IC) and the corresponding time-course.....	50
Figure 4.2:	The output of GIFT software showing an independent component, its corresponding time-course and frequency spectra.....	51
Figure 4.3:	The output of GIFT software showing an independent component, its corresponding time-course and frequency spectra.....	52
Figure 4.4:	The architecture of the designed convolutional autoencoder for obtaining functional connectivity patterns.....	54
Figure 4.5:	Loss curve for the convolutional autoencoder during the training.....	54
Figure 4.6:	One sample of synthetic connectivity matrices from each pattern.....	56
Figure 4.7:	Visualization of the synthetic connectivity matrices using t-SNE.....	57
Figure 4.8:	T-SNE visualization of the latent representations of the generated connectivity matrices obtained by the designed CAE	58
Figure 4.9:	Average of the correlation matrices in each state.	60
Figure 4.10:	Median of correlation matrices in each state for the healthy control subjects	61
Figure 4.11:	Median of correlation matrices in each state for the schizophrenia patients.	62
Figure 4.12:	Two-sample t-test results showing FC differences between pairs of the brain regions in the healthy control (HC) subjects and corresponding brain regions in the schizophrenia (SCZ) subjects in each state obtained by using the proposed clustering method.....	64

Figure 4.13: The regions in the visual network part of the brain where significant differences exist between those in groups of HC and SCZ65

Figure 4.14. Two-sample t-test results showing FC differences between pairs of the brain regions in the healthy control (HC) subjects and corresponding brain regions in the schizophrenia (SCZ) subjects in each state obtained by using the traditional clustering method of k-means..66

Figure 4.15: Average dwell time in each state for the HC and SCZ group.....67

Figure 4.16: Average dwell time in each state for the HC and SCZ groups after applying traditional k-means clustering method.....68

List of Tables

Table 4.1:	Summary of subject demographic	46
Table 4.2:	Convolutional autoencoder layers.....	55
Table 4.3:	Number of matrices in different clusters	59

List of Symbols

A	Mixing matrix
A_i	Coefficient corresponding to the component S_i
C	Inverse of the matrix A
D	Number of sliding windows
F_i	Reducing matrix determined by PCA (Subject-level)
f	Filter size (Kernel size)
G_i	Reducing matrix determined by PCA (Group-level)
K	Number of clusters
L	Number of rows in a dimension-reduced fMRI data
M	Number of subjects
N	Number of independent components
S	Matrix of independent components
O	Output of a neural network
p	Padding size
q	Stride size
S_i	i^{th} independent component
T	Number of signals (Number of fMRI scans)
V	Length of each signal
W	Length of the sliding window
w_{ij}	Weight between neuron i and j

X	Matrix of data
Y	Dimension-reduced fMRI data of a subject
α	Learning rate
\emptyset	Activation function
τ	Time shift of the sliding windows

List of Abbreviations

ANN	Artificial Neural Network
AU	Auditory
BOLD	Blood Oxygen Level Dependent
CAE	Convolutional Autoencoder
CB	Cerebellum
CC	Cognitive Control
CNN	Convolutional Neural Network
CSF	Cerebrospinal Fluid
DMN	Default Mode Network
EEG	Electroencephalography
FC	Functional Connectivity
FMRI	Functional Magnetic Resonance Imaging
FOV	Field of View
ICA	Independent Component Analysis
MEG	Magnetoencephalography
MNI	Montreal Neurological Institute
MRI	Magnetic Resonance Imaging
PCA	Principal Component Analysis
RELU	Rectified Linear Unit
ROI	Region of Interest
RSN	Resting State Network

SC	Subcortical
SPM	Statistical Parametric Mapping
SM	Sensorimotor
T-SNE	T- Distributed Stochastic Neighbor Embedding
TR	Time to Repetition
VIS	Visual
WM	White Matter

CHAPTER 1: Introduction

1.1 Background

Functional MRI (fMRI) has the potential to open novel insights to the understanding of the brain functions. It is considered to be a noninvasive and safe technique for visualizing and mapping functional brain activity. Functional MRI is also used to investigate the connectivity patterns among the different brain regions. This functional connectivity study can be carried out using fMRI in resting-state or during task-related experiments. In this thesis, we focus on the functional connectivity in resting-state fMRI. Functional connectivity (FC), which is the correlation between activation signals of different brain regions, has been assumed for a long time to have a stationary nature. It has been only recently that the dynamic behavior of FC is revealed, showing the functional connectivity between different brain regions have meaningful variations in resting-state fMRI [1]. Therefore, some works have been done to assess and characterize the dynamic FC (dFC) in order to explore how the brain functions in healthy people and in people with different psychological disorders.

In order to study the functional connectivity using fMRI data, it is necessary to understand the basis of the brain structure and the functional imaging tool.

1.2 Human Brain

Brain is the most complex organ inside human body that has billions of nerves communicating through passing electrical signals at junctions called synapses. Anatomically, brain tissue consists of grey matter (GM) and white matter (WM). The grey matter that includes neuron cell bodies and dendrites is responsible for the most of high-level brain functional processes. The white matter

that consists of bundles of long myelinated axons is responsible for transferring of the information to different grey matter regions. There is also a clear liquid in the brain and spinal cord called cerebrospinal fluid (CSF) [2]. Figure 1.1. (a) and Figure 1.1. (b) demonstrate a typical neuron in human brain and a vertical cut of the brain, respectively.

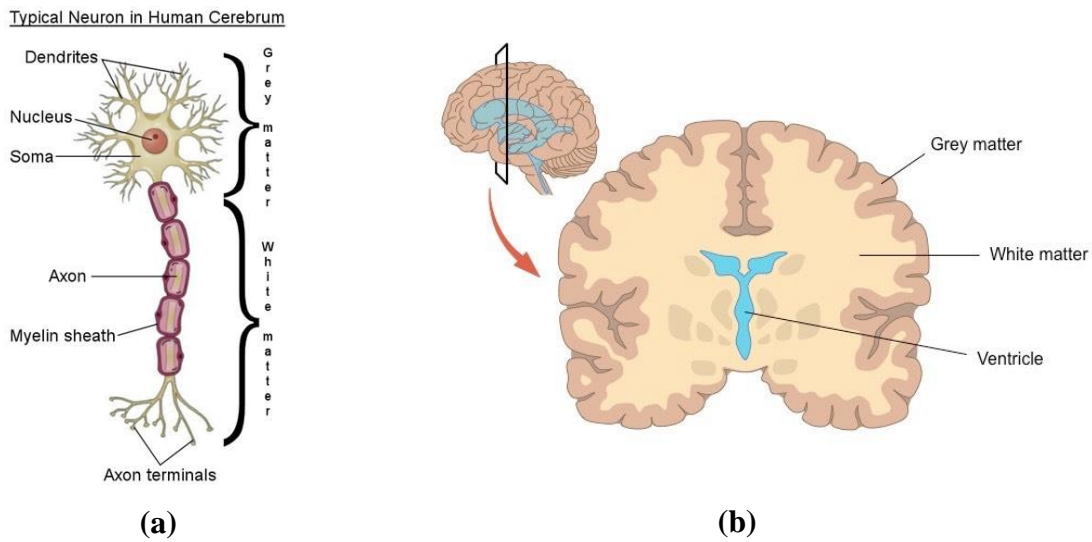


Figure 1.1. a) The structure of a typical neuron in human brain [3]. b) A vertical cut of brain showing grey matter and white matter tissues [4].

1.3 Functional and Anatomical Brain Connectivity

Our brain is a network of many different brain regions. Each brain region is specialized in performing specific tasks and functions. Structural connections in the brain mainly refer to anatomical pathways that directly interconnect spatially separated brain regions. Diffusion tensor imaging (DTI) is an imaging technique for visualizing anatomical connections [5] as shown in Figure 1.2. (a). On the other hand, the functional connectivity is defined as the pattern of temporal correlation made by the interactions between segregated brain region pairs [6]. In other words,

functional connectivity shows the statistical relationship between the signals of different brain regions. Study of the functional connectivity among brain regions can be done by using the functional magnetic resonance imaging (fMRI). Figure 1.2. (b) illustrates an example of functional map showing the relationship between the activity of brain regions.

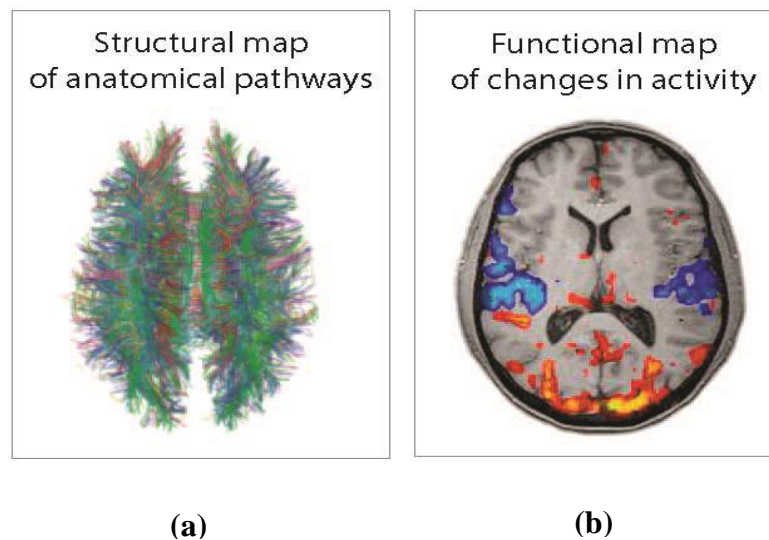


Figure 1.2. a) White matter fiber tracking using DTI. b) Functional connectivity map showing the coactivation between some brain regions [7].

1.4 Functional MRI

Functional magnetic resonance imaging (fMRI) is an imaging tool providing a high spatial resolution, noninvasive and safe technique for visualizing and mapping the functional brain activity. It is used in a growing number of studies [8-11] to understand the functionality of a human brain and to explore interaction, connection and coordination of different parts of the brain. It is also used to study the differences in the brain functionality of healthy people and people affected by some psychiatric brain disorders [12-14].

The basis of the fMRI sensitivity to the brain neural activity arises from the local magnetic field changes. Oxygenated and deoxygenated blood have different paramagnetic properties. In contrast to deoxygenated blood that is paramagnetic, oxygenated blood is diamagnetic i.e. it causes almost no effect on the magnetic field. Upon neural activation of a local brain area, blood flow increases in order to provide more oxygen and glucose to that area. Consequently, the blood deoxyhemoglobin concentration decreases, as shown in Figure 1.3. This causes a distortion in the magnetic field and an increase in the blood-oxygen-level dependent (BOLD) signal. In fMRI, the contrast in the BOLD signal is used to observe the different areas of the brain, activated at a given time [15, 16].

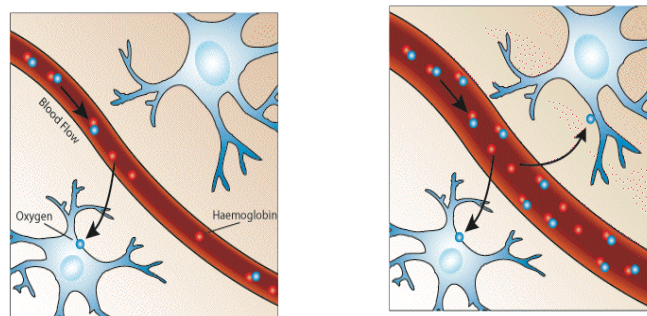


Figure 1.3. Increase in blood flow resulted from brain neural activity leads to increasing glucose and oxygen and decreasing in deoxyhemoglobin [17].

Compared with other methods, such as EEG and MEG, fMRI provides a higher spatial resolution and thus has got a lot of interest from researchers [8-11]. In fMRI, scans of the whole brain are acquired over time. Each scan includes slices of the brain volume. The time resolution (TR) is defined as the time between two sequential scans of the same point in the brain. The temporal resolution (TR) is usually 2–3 seconds. Each scan of fMRI is a three-dimensional image (a 3D volume) and the term voxel is referred to an element of this 3D volume. The value of each voxel

changes from one scan to another scan over time. Hence, as shown in Figure 1.4, fMRI is a 4D data where three dimensions are used to reconstruct voxels in the space and fourth dimension (time) measures the activation of each voxel over time.

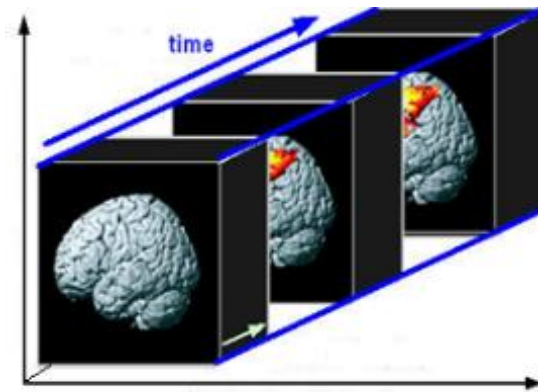


Figure 1.4. fMRI data as a time sequence of 3D images [18].

1.5 Resting-State fMRI

Brain consumes 20% of the energy in the body during spontaneous brain activity. Only a small percentage of the energy consumed by the brain is used for task-related activities [19]. In view of this, study of the resting-state fMRI is shown to be important. In the resting-state fMRI, a subject who lies inside the fMRI scanner is trained to let his mind wonder without doing any specific task. In contrast, there is another type of study for task-related fMRI that tries to find spatial activation pattern of human brain when a subject performs a cognitive task. Figure 1.5 illustrates an fMRI scanner where a subject lies inside it.

Biswal *et al.* [20] were the first researchers who found out that the left and right hemispheric regions of the primary motor network show a high synchronization between their BOLD time courses during resting-state experiment. Since then, researchers have been able to map the intrinsic functional connection diagram of brain without using any designed tasks and resting-state studies have received lots of attention [21, 22]. Also, the resting-state fMRI allows researchers to study the brain function of patients who are not able to do complicated tasks or long experiments. In contrast to the task-based functional imaging that typically highlights a single brain region associated to any given task, the resting-state fMRI highlights the activity among different brain regions at once. Hence, study of the resting-state fMRI is valuable for varieties of research topics including the study of psychological brain disorders [14]. The resting-state fMRI can also be used to study and compare the functional activities in the different brain regions of two different groups, such as patients with Schizophrenia and healthy subjects [23].

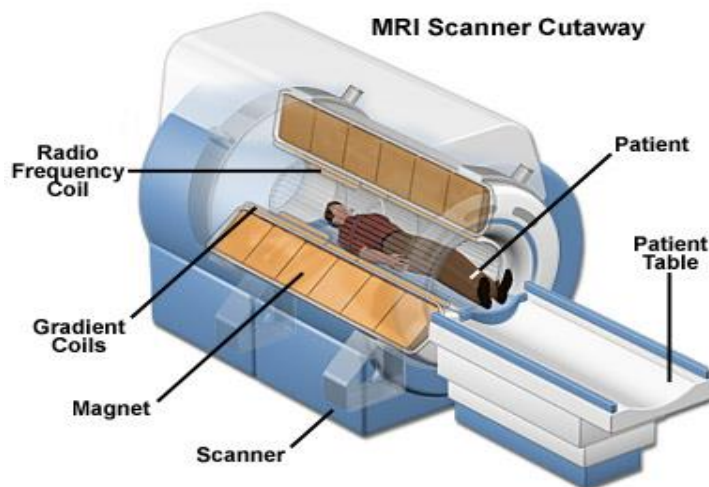


Figure 1.5. A fMRI scanner; a functional magnetic resonance imaging equipment with a strong magnetic field to measure brain activity [24].

1.6 Resting-State Networks

It has been shown in the resting-state functional studies that there are some groups of brain regions in which a strong functional connectivity exists. In other words, these regions activate and deactivate together during rest. These brain regions are the same across all subjects and are referred to as resting-state networks (RSNs) [21, 22]. Default Mode, Visual, Auditory, Cognitive Control/Attention, Sensorimotor and Cerebellum are some of the most common RSNs in different studies, their locations in the brain are shown in Figure 1.6.

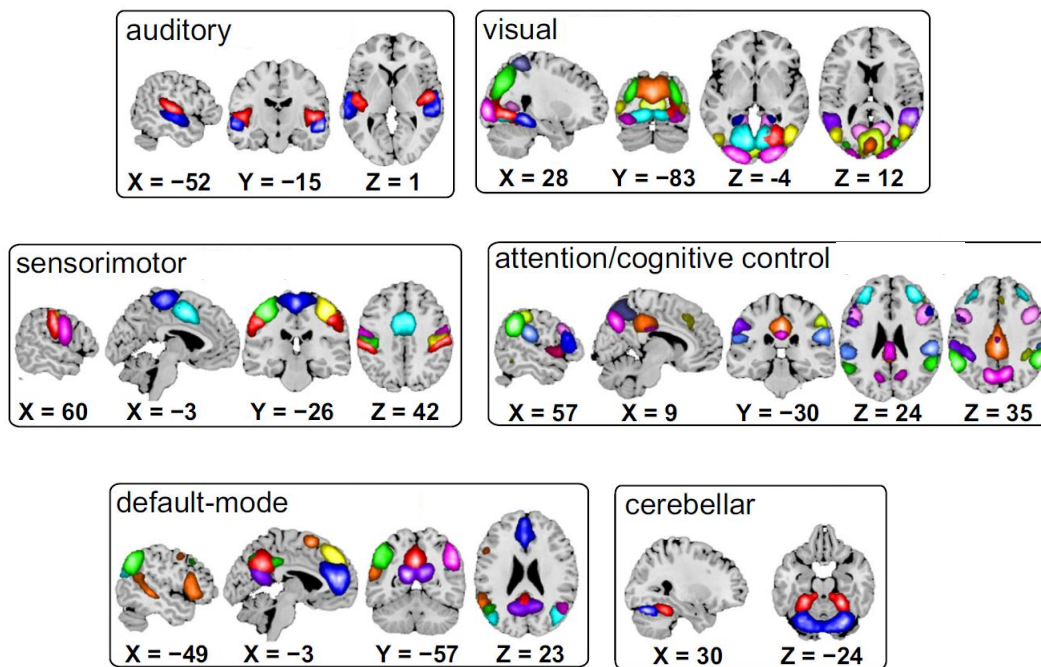


Figure 1.6. Common resting-state networks [25].

1.7 Static and Dynamic Functional Connectivity

Study of the functional connectivity (FC) can be carried out by considering FC to be static or dynamic. Static functional connectivity is obtained by finding the correlation between activation signals of different brain regions over the course of many minutes, assuming the FC does not

change in time. Although the static functional connectivity provides useful information, many years of research has shown that the brain activity is not constant and varies in time [26-28]. In view of this, finding the correlation between the activation signals of different brain region pairs across 5-10 minutes of fMRI recording results in losing a lot of information about their functional connectivity. Hence, the functional connectivity should be measured within time in a dynamic way. The dynamic functional connectivity is measured by obtaining the time-varying correlation between activation signals of different brain region pairs within fMRI recording time. There are different methods for analyzing fMRI functional connectivity. Generally, these methods are grouped into two types: model-based methods and data-driven methods [29].

1.8 Functional Connectivity Analysis

In many studies [30-32], the analyses of the functional brain connectivity are carried out by using the model-based approaches. In the model-based analysis, the connection between the regions of interest (ROI) is calculated by using some matrices, such as cross-correlation to generate the functional connectivity map of the human brain. Selecting the regions of interest needs some prior knowledge about the anatomy of brain. By using the model-based analysis, we need to make decisions on the size, shape and location of the regions of interest that may lead to the different outcomes in the functional connectivity analysis.

On the other hand, there are some data-driven approaches that are based on the features extracted from the input data (fMRI data). The advantage of using these approaches is that they do not require a prior selection of the brain regions and are able to decompose the captured fMRI data into a set of separated brain regions. It is helpful to evaluate the functional connectivity in fMRI data without considering any prior information about its spatial or temporal pattern. The most

commonly used methods to achieve such a decomposition are independent component analysis (ICA) and principle component analysis (PCA) [21,29].

1.9 Brief Literature Review Survey

Assessment of the functional connectivity using the resting-state fMRI underlines specific information across the whole brain. The recent studies have shown that the functional brain connectivity in the healthy people is different from that in the people affected by mental diseases [11,12,13,22]. For many years, researchers have studied the static functional connectivity assuming the temporal dependency among different brain regions is global and constant during a few minutes of resting-state fMRI recording [33, 34]. However, other studies using high temporal resolution techniques such as electroencephalogram (EEG) and magnetoencephalography (MEG) have shown the problem with this assumption and have observed that there are spontaneous changes in the brain activity [35, 36]. Hence, the assumption of the functional connectivity being static and constant during a resting-state fMRI experiment is an over-simplification despite its convenience. Given the increasing evidence on the importance of dynamic functional connectivity in the resting-state fMRI for assessing intrinsic function of the brain, the researchers' focus has shifted from static functional connectivity to time-varying or dynamic functional connectivity. The study by Allen *et al.* in 2013 [8] is one of the first major works on time-varying functional connectivity, usually referred to as dynamic connectivity, using resting-state fMRI. In this study, the assessment of the whole-brain dynamic functional connectivity was investigated employing three major steps. First, a data driven technique (spatial independent component analysis) is applied to the fMRI data to decompose it into independent components and the corresponding time courses. In the second step, by passing a sliding window through time-courses, correlation matrices that show the degree to which each region is correlated with other regions of brain are obtained.

Finally, the correlation matrices are clustered for the purpose of studying the dynamic properties of functional brain connectivity. There are some other studies based on the pipeline proposed in [8] to investigate the dynamic functional connectivity in different brain diseases including the work done by Yao *et al.* [38,39] and [40] for studying the time-varying functional connectivity in autism and bipolar disorder, respectively. The limitation of the proposed procedure in [8] for finding the dynamic functional connectivity is that the clustering of the correlation matrices for capturing different dynamic functional connectivity patterns has been carried out by k-means method. However, the k-means method has been shown to be suboptimal for being applied to the high dimensional data. In 2015, Yaesoubi *et al.* [37] proposed a novel pipeline to characterize the functional interactions among the different brain regions using time-frequency analysis. One advantage of the pipeline proposed in [37] over the one in [8] is that there is no need to exploit the sliding windows to capture the dynamic functional connectivity. However, the problem with the proposed method in [37] is that the interpretability of the functional connectivity results is so difficult in time-frequency domain. Hence, the pipeline proposed in [8] is more dominant in neuroscience community for studying the dynamic functional connectivity in the healthy and diseased brains using the resting-state fMRI. It should be noted that the proposed method in [37] also has the same limitation as [8] that is the use of k-means for clustering the different functional connectivity patterns.

1.10 Motivation and Thesis Objective

As mentioned in previous section, applying the k-means clustering to the functional connectivity matrices for finding the reoccurring functional connectivity patterns is one of the common steps in most of the works [8, 37, 38, 40]. In general, the k-means clustering is a suitable option for the

clustering of low dimensional data. However, this method does not perform well for high dimension data such as images. It is resulted from the fact that using Euclidian distance over high dimensional spaces (such as images with lots of pixels) is not intuitive. An example of high dimensional data is the 28×28 images of MNIST handwritten digits in which the k-means has been shown to fail in clustering them properly [41]. In view of this, we concluded that applying the k-means method to the correlation matrices for finding the connectivity patterns (as done in most of the other works) is not optimal and can lead to an inaccurate result. In this thesis, as the main contribution we address this issue by using a convolutional autoencoder for obtaining the correlation matrices with the common functional connectivity patterns. By using these connectivity patterns, we can study the differences between the functional brain connectivity in the healthy control subjects and that in patients.

1.11 Organization of the Thesis

This thesis is organized as follows. In Chapter 2, the background materials used in this thesis for studying the functional brain connectivity are presented. This chapter is divided into three main parts. In the first part, the preprocessing steps that are typically applied to the raw fMRI data for reducing the artifact and noise are explained. In the second part, the theoretical background about the independent component analysis and its extension, called group ICA are presented. Then, we explain about applying the group ICA to the fMRI images and obtaining the correlation matrix from pairwise correlation between time-courses corresponding to independent components. In the last part of Chapter 2, we explain the process of obtaining the dynamic functional brain connectivity using sliding windows. In Chapter 3, the whole procedure for obtaining the dynamic functional connectivity in this study is presented. The Chapter 3 is divided into two main parts. In

the first part, the neural networks and convolutional autoencoders for extracting latent representations are explained. In the second part of the chapter, for the first time, we propose using the convolutional autoencoders for obtaining the dynamic functional brain connectivity patterns. In Chapter 4, the procedure developed in Chapter 3 is applied to the data gathered from 72 healthy control subjects and 74 patients affected by schizophrenia. After following the procedure given in Chapter 3, including the preprocessing, group ICA and using the convolutional autoencoder for clustering the connectivity matrices, a two-sample t-test is performed on each cluster in order to determine each pair of the brain regions in the group of the healthy control subjects for which the correlation value is significantly different from that of the corresponding pair of in the group of patients.

CHAPTER 2: Background Material

2.1 Introduction

In this chapter, the background materials that are directly linked to study of the functional brain connectivity are presented. First, the preprocessing steps for fMRI data is explained in detail in Section 2.2. In Section 2.3 and 2.4, the concept of independent component analysis (ICA), its statistical characteristics and its usage for the extraction of fMRI components are described. Next, in Section 2.5 group ICA method for overcoming the limitation of ICA in the group study of fMRI data are explained. Selecting the suitable ICA components (output of group ICA) and excluding the artifact components is then discussed in Section 2.6. In Section 2.7, the framework for obtaining the dynamic functional brain connectivity is presented. Finally, the two-sample t-test method for finding the group differences is described.

2.2 Preprocessing of fMRI Images

In order to reduce the artifact and noise in the fMRI data, preprocessing procedures are commonly applied to raw functional MRI data prior to applying any other statistical method. The common preprocessing steps, including slice timing correction, realignment, coregistration, normalization and spatial smoothing are explained in detail in the following subsections.

2.2.1 Slice Timing Correction

In fMRI, scans of the whole brain are acquired over time. Each scan itself includes slices of the brain volume. These slices are not acquired at the same time. For example, for a scan of 30 slices and a TR of 3 seconds, the last slice is taken 3 seconds after the first slice. Since for analyzing the

fMRI data, the assumption is that all the slices of each scan are acquired at once, slice timing correction preprocessing step is exploited to overcome the problem of time differences among the slices in a scan. In more detail, in this preprocessing step, one of the slices of each scan (commonly the middle slice) would be considered as the reference slice, all the other slices of its corresponding scan would be shifted in time according to the reference slice as shown in Figure 2.1. Hence, after applying time-slicing correction to the fMRI data, all the slices in each scan can be considered to be acquired at the same time.

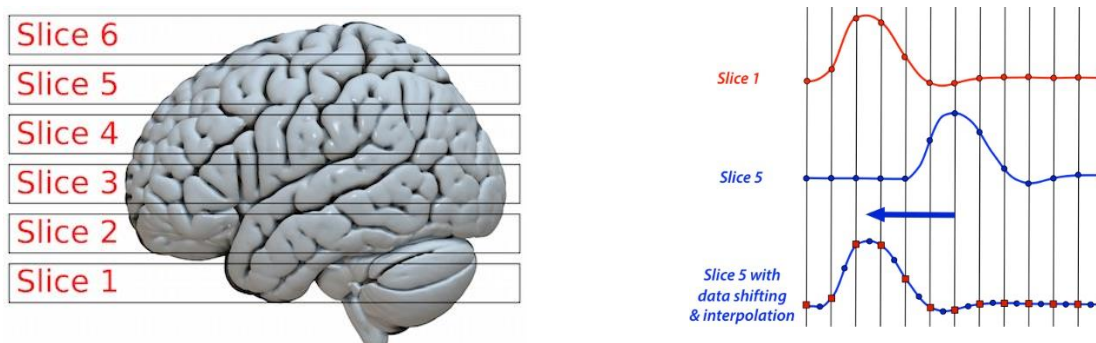


Figure 2.1 Time slicing, a preprocessing step for fMRI data [42, 43].

2.2.2 Realignment

Another preprocessing step applied to the fMRI data is realignment. During the recording of the fMRI data, subjects might move their head slightly. It can result in adding noise to the fMRI data and consequently making the analysis of fMRI data difficult. During analysis of fMRI data, we have to make sure that a time course represents values from the same voxel location in each fMRI scan. Hence, the head movement problem should be addressed by applying the realignment procedure to the fMRI data prior to starting the fMRI analysis. In the realignment procedure, the difference between consecutive slices of fMRI images are minimized and the slices are aligned by using 6 parameters (3 translations in X, Y and Z directions and 3 rotations around the X, Y and Z

axes), so that all the slices would have the same orientation. Figure 2.2 shows the realignment of the slices in a scan of the fMRI data.

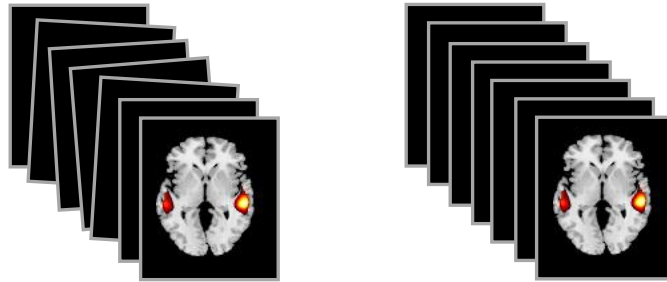


Figure 2.2 Realignment of slices.

2.2.3 Coregistration

Coregistration is another important step in the preprocessing of fMRI data. Coregistration refers to the alignment of the functional images to the structural image from the same subject brain by maximizing the mutual information. An example of the coregistered anatomical and functional fMRI data are shown in Figure 2.3. As the result, the coregistration is useful for visualizing the brain activation on a higher spatial resolution image of the brain.

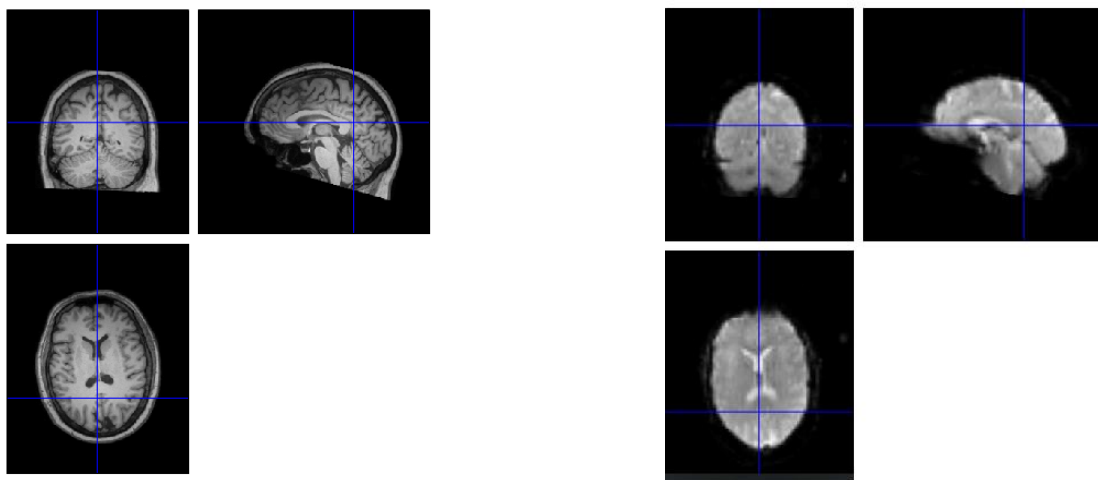


Figure 2.3 Coregistration, aligning the functional MRI data with structural image.

2.2.4 Normalization

Normalization is an important preprocessing step that is applied to the fMRI data after coregistration. Since people have different shape of brain, the normalization step is required for aligning the fMRI data of different subjects to a standard template such as the one shown in Figure 2.4 that is Montreal Neurological Institute (MNI) space. The MNI template is obtained from taking the average of brain anatomical images of 152 subjects. After transforming the fMRI data of all subjects into the same space, the location of a voxel remains the same across all the subjects. Hence, after applying the normalization, we are able to compare the fMRI data across subjects.

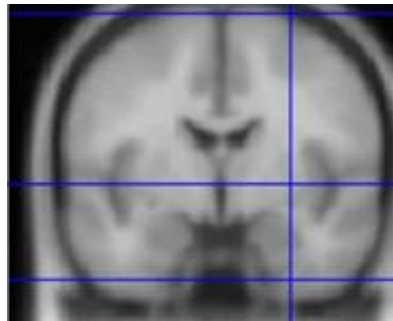


Figure 2.4 MNI space, averaged anatomical images of 152 subjects [45].

2.2.5 Spatial Smoothing

The last preprocessing step for fMRI data is spatial smoothing. In the spatial smoothing step, the main goal is to remove the high frequency noise and artifact from fMRI data. For this purpose, a gaussian kernel is spatially convolved to the fMRI images in order to increase the signal to noise ratio. After convolving a gaussian kernel with the image, the value at each voxel will be replaced by a weighted average of the values in surrounding voxels.

After applying the above-mentioned preprocessing procedures to the fMRI data, the resulting fMRI data are prepared for further analysis, such as applying ICA.

2.3 Independent Component Analysis

Independent component analysis (ICA) is a statistical method used to extract unknown source signals from their linear mixtures based on an assumption that the source signals are statistically independent and non-gaussian [46]. In other words, ICA tries to decompose a data into a linear combination of the independent source signals (independent components) without having any prior information about these source signals. A classic example of ICA is shown in Figure 2.5.

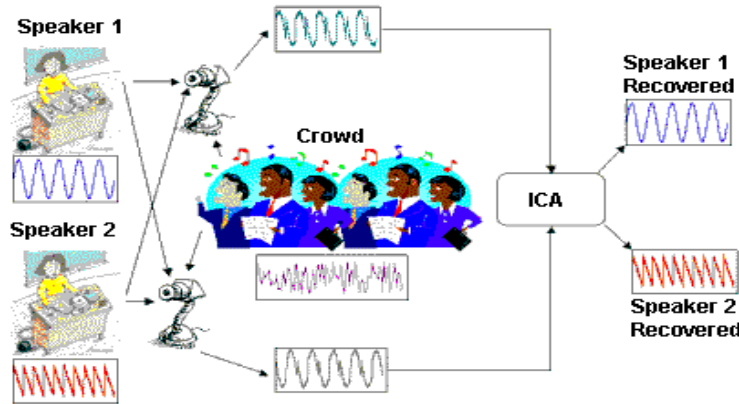


Figure 2.5. Separating mixed speech data recorded by microphones using ICA [47].

If our data consist of T signals, each with length V , we can arrange them into a matrix $X_{T \times V}$ with T rows and V columns. Then, by applying ICA, the data decomposes to N independent component as shown bellow

$$X = AS = \sum_{i=1}^N A_i S_i \quad (2.1)$$

where S is a $N \times V$ matrix, S_i is the i^{th} row of matrix S (i^{th} independent component) and A is a $T \times N$ mixing matrix. The i^{th} column of A , A_i , represents the coefficients corresponding to the component S_i . It should be noted that we only observe the data X , and both A and S need to be estimated.

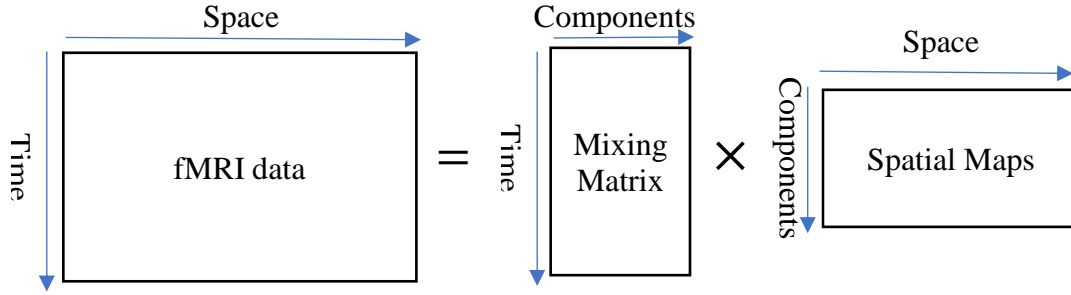


Figure 2.6. Applying ICA to fMRI data.

The matrix S can be obtained by multiplication of matrix X by matrix W as

$$S = CX \quad (2.2)$$

where C is the inverse of the matrix A . Hence, a linear combination of the x_i, x_i is the i^{th} column of X , can estimate one of the independent components. In other words, if c be one of rows of C , $y = c^T x$ is a linear combination that result in one of the independent components. According to the central limit theorem the distribution of sum of independent random variables is closer to gaussian distribution than the distribution of the original variables. In order to estimate c , we first consider a change of parameter as $z = A^T c$ so that $y = c^T x = c^T A s = z^T s$. Based on the central limit theorem, $z^T s$ is more gaussian than any of the s_i and the gaussianity of $z^T s$ is minimized when it equals to one of the independent components (s_i). In other words, taking c to maximize the nongaussianity of $c^T x = z^T s$ is equivalent to have the vector z with only one non-zero element. In this case, $c^T x$ gives one of the independent components [45]. Quantitative measures of the non-gaussianity for ICA estimation are using kurtosis, negentropy and approximation of negentropy.

For example, in FastICA, a popular algorithm for estimation of independent components, non-gaussianity is maximized by using the approximation of negentropy which is faster and more robust than kurtosis. Another approach for estimation of independent components in ICA is minimization of mutual information that is shown to be equivalent to maximizing the nongaussianity. In the Infomax ICA algorithm that is one of the most popular ICA algorithms, the independent components are estimated by minimizing the mutual information.

2.4 ICA in fMRI

Since in the resting state fMRI we have no prior information in time and in location, there is an increasing interest in applying ICA algorithm to the resting-state fMRI data for studying the spatial and temporal properties of fMRI data [8, 21, 23, 25, 26, 38, 48]. ICA works based on an assumption that BOLD fMRI time series are generated by linear mixture of neural activities.

There are two approaches for applying ICA to achieve maximal independence components in space or in time for analyzing fMRI data. 1- Spatial ICA, which extracts independent spatial images and a set of corresponding time courses, 2- temporal ICA, which extracts independent time courses and a corresponding set of images [49]. Analysis of spatially independent components is by far the most common approach in fMRI studies. In our work, the application of ICA is to determine spatially separate brain regions and their corresponding time courses with aim to studying functional brain connectivity. Therefore, spatial ICA, is more appropriate for the task of this research. A schematic representation of the spatial ICA applied to the fMRI data is shown in Figure 2.7.

As explained in chapter 1, fMRI data is a 3D data (scan) at any given time. In order to prepare our data, we can flatten each of these scans and put it into a row of a matrix, X . Hence, each row in

matrix X represents all the voxels of a fMRI scan at a fixed time point and each column represents a single voxel time series. The matrix X is a T by V matrix, where T and V are the number of time points and the number of voxels in a fMRI scan, respectively. ICA decomposes the matrix X (the original fMRI data) into an independent component matrix S and its respective mixing matrix A as shown in Figure 2.7 by maximizing the statistical independence of the estimated components through an iterative optimization procedure.

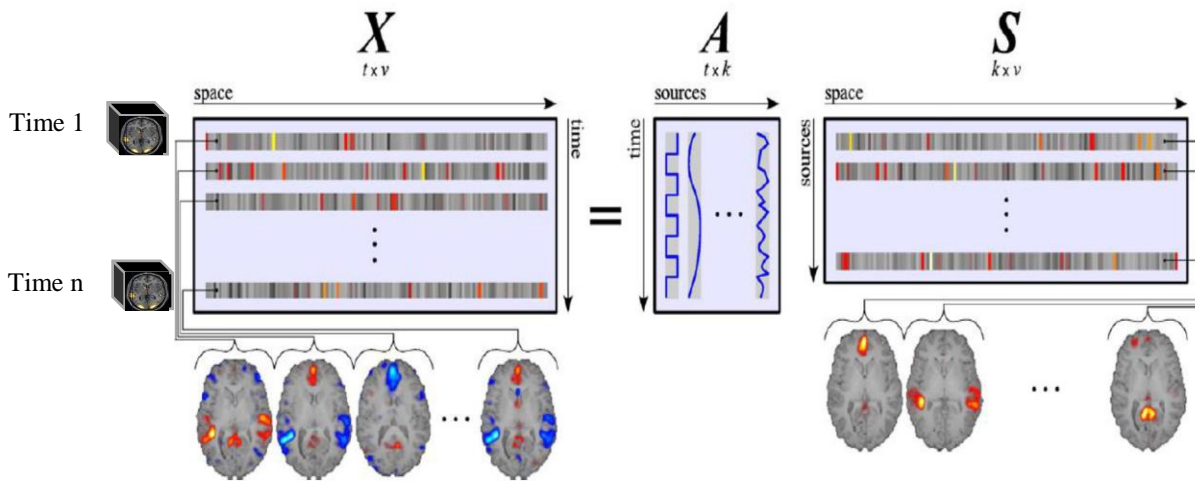


Figure 2.7. Decomposition of fMRI images using ICA. Each row of X is a scan of brain flattened at a certain time point; Each column of A is a coefficient (time course) of the corresponding component; Each row of S is an independent component [50].

S is a $N \times V$ matrix (N is the number of components and V is the number of voxels in each scan) and S_i is the i^{th} independent component of fMRI data. Matrix A is a $T \times N$ mixing matrix and each column of A with length T is called the time course corresponding to i^{th} IC in matrix S (s_i). Therefore, there is a time course corresponding to each independent component. The statistical relationship between each pair of the time-courses specifies the functional connectivity between the corresponding pair of the components.

2.5 Group ICA

ICA is suitable to be applied to a single subject fMRI data. However, the problem with using ICA in fMRI data comes from the arbitrary order of the obtained components for each subject. Hence, the result of the individual ICA applied to each subject's fMRI data does not directly correspond to that of the ICA applied to other subjects' fMRI data. However, the components correspondence across all the subjects is necessary for statistical analysis and multi-subject studies. Group ICA (GICA) has been proposed in 2001 by Calhoun *et al.* [48] to solve the problem of establishing subject correspondence in group studies.

Prior to applying group ICA to fMRI data, two levels of data-reduction are carried out to reduce the computational burden. These two data reduction steps are done by using principal component analysis (PCA) method. The first data reduction step is done to reduce the dimension of the data for each individual subject (performing a subject-level PCA). After dimension reduction of each subject's functional MRI data, the dimension-reduced data of the different subjects are vertically concatenated into one single matrix as shown in Figure. 2.8. Then, another data reduction step is applied to the concatenated matrix (performing a group-level PCA) [48].

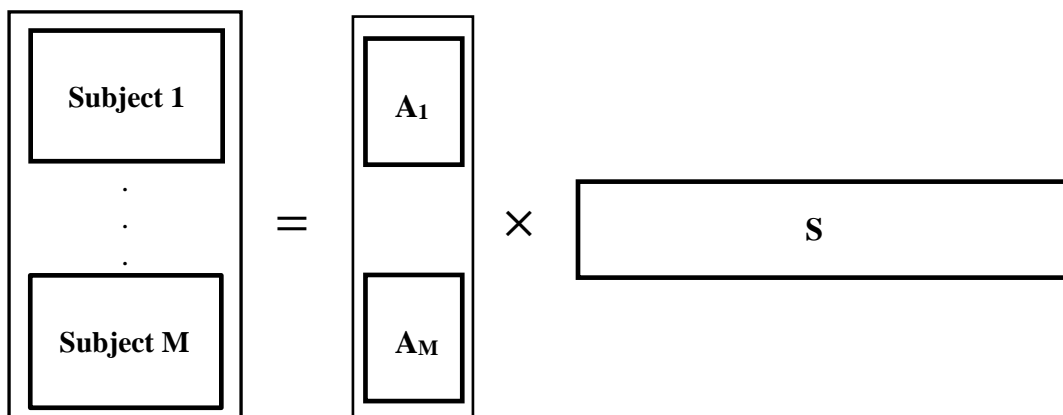


Figure 2.8 Applying ICA to the concatenated dimension reduced data of different subjects.

To explain the procedure in more detail, assume there are M subjects. Let Y_i be a L -by- V dimension-reduced data matrix from subject i and it is obtained by multiplication of matrix X_i by F_i , where X_i and F_i are the T -by- V preprocessed data matrix (spatially normalized data), and the L -by- T reducing matrix (determined by the PCA decomposition), respectively.

$$Y_i = F_i X_i \quad (2.3)$$

In terms of fMRI data, V is the number of voxels, T is the number of fMRI time points, and L is the size of the time dimension following reduction.

After vertical concatenation of M dimension-reduced subject data, a second-level PCA is applied at the group level to reduce the dimension to N (the number of components to be estimated).

$$Y = G \begin{bmatrix} F_M X_1 \\ \cdot \\ \cdot \\ \cdot \\ F_M X_M \end{bmatrix} \quad (2.4)$$

where G is an $N \times LM$ reducing matrix determined by a PCA decomposition. This matrix G is multiplied by the $LM \times V$ concatenated data matrix for the M subjects to obtain $N \times V$ reduced matrix. This matrix is then used in the ICA estimation stage.

After carrying out ICA estimation, Y would be decomposed as AS where A is the $N \times N$ mixing matrix and S is the $N \times V$ component map. By substituting this expression for Y into Equation 2.4 and multiplying both sides of Equation 2.4 by G^{-1} , we have

$$G^{-1}AS = \begin{bmatrix} F_1 X_1 \\ \cdot \\ \cdot \\ \cdot \\ F_M X_M \end{bmatrix} \quad (2.5)$$

If we partition the matrix $G^{-1}A$ by referring to each subject, we have the following expression

$$22 \quad (2.6)$$

$$\begin{bmatrix} G_1^{-1}A_1 \\ \cdot \\ \cdot \\ G_M^{-1}A_M \end{bmatrix} S = \begin{bmatrix} F_1X_1 \\ \cdot \\ \cdot \\ F_MX_M \end{bmatrix}$$

Then, the equation for subject i can be written such that

$$G_i^{-1}A_iS = F_iX_i \quad (2.7)$$

We now multiply both sides of Equation 2.7 by F_i^{-1} and write

$$X_i = F_i^{-1}G_i^{-1}A_iS \quad (2.8)$$

Equation 2.8 provides the ICA decomposition of the data, X , for subject i . The N -by- V matrix S contains N independent components and the $F_i^{-1}G_i^{-1}A_i$ matrix is the single subject mixing matrix. In other words, back-reconstruction allows projecting group-level ICA results at the single subject level.

After estimation of independent components and obtaining subject-level time-courses a post-processing step need to be done to remove unsuitable components.

2.6 Component Selection

The fMRI data contain a lot of noise and artifacts resulted from heart-beat, breathing, head motion and the MRI acquisition system. After applying the group ICA to the fMRI data for obtaining the independent components, each component needs to be evaluated and the problematic components resulted from the artifacts in fMRI data should be excluded. In other words, in order to select the best components of the fMRI data, all the independent components and their corresponding time courses are required to be visually inspected. There are two main criteria for selecting the proper independent components of fMRI data for further analysis as follow,

1) Spatial feature of component

The independent component (IC) spatial maps should be inspected visually for us to be able to decide on keeping or excluding each component. First, the independent components and their peak activations should be in grey matter (GM) area for being qualified to be considered as the proper components. In other words, the components located in white matter (WM), cerebrospinal fluid (CSF) or those having overlap with brain arteries should be excluded. Also, the components located near brain edges and those with ring-like shape are due to the head motion artefact and should be excluded in the component selection process [51].

2) Time-course and power spectra

Inspecting the time-courses (TCs) corresponding to the independent components can also help us to find out which independent components are resulted from the artifact and should be excluded. In BOLD signals, the highest power is between 0.01 - 0.1 Hz. Hence, one of the main criteria to decide if a time-course indicates a BOLD-related signal is to inspect the presence of low frequency power. Power spectra of TCs should exhibit low frequency power with presence of the highest power between 0.01 – 0.1 Hz. However, sometimes the physiological noise due to cardiac pulsation (~ 1 HZ) or respiratory cycles (~ 0.3 HZ) becomes aliased into the low frequency fMRI time-course [51].

2.7 Dynamic Functional Brain Connectivity

The simplest way to investigate the degree to which each component is functionally related to the other components is to capture the pairwise Pearson correlation between the corresponding time-courses. By considering N different brain components, a $N \times N$ symmetric matrix of connectivity can be obtained. Each element of this matrix is the correlation value between the time-courses of each pair of the components. Figure 2.9 shows an example of a connectivity matrix. Since the matrix of connectivity is a symmetric matrix, it has $N \times (N - 1)/2$ unique features. In connectivity matrix, the components based on their functional and anatomical location are grouped to form some networks such as auditory network, visual network, sensorimotor network and so on. The positive value of the correlation between the time-courses corresponding to a pair of brain regions is shown by the red color in Figure 2.9. Also, the negative correlation is represented by the blue color. If we calculate the correlation between the whole length of the time-courses corresponding to each pairs of the brain regions, the resulting correlation matrix would show the static functional connectivity.

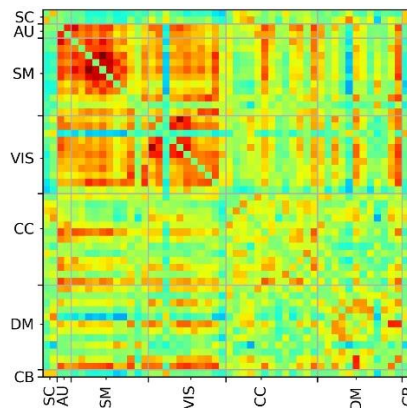


Figure 2.9. An example of the brain functional connectivity matrix. The independent brain components are separated into seven groups. Sub-cortical (SC), auditory (AUD), visual (VIS), sensorimotor (SM), cognitive control (CC), default mode (DM) and cerebellum (CB).

As mentioned before, by studying the static functional connectivity, we are unable to understand the changes in the functional connectivity within the time. In 2013, Allen *et al.* [8] published one of the first major works on capturing dynamic functional brain connectivity. In this work, the functional connectivity was measured by using a set of temporal windows. Hence, for obtaining dynamic functional connectivity, a sliding window was applied to the time-courses, and then the correlation matrix was calculated inside each window as shown in Figure 2.10. In other words, first, by considering the length of window as W , the correlation matrix is calculated from time $t = 1$ to time $t = W$. Then, by shifting the window by time τ repeatedly, the same calculation is carried out in each window over the time, from the beginning of time-courses to the end of the time-courses. Considering length of window W to be too short leads to the reduction of the signal to noise. It also results in having few samples for a reliable computation of correlation. In contrast, by having the long window length, we would not be able to detect the temporal changes in dFC. In other words, the length of window must be short enough to capture all the variations in dFC and long enough to get the reliable information of correlation. The size of 30–60s for the windows are suggested by the most studies for capturing the changes in resting-state dFC [1]. It also has been shown that, in most cases, different window lengths, when chosen in this interval, do not give significantly different results. Beside choosing the window length, defining the shape of the window is important. The most basic window is the common rectangular window. The limitation of using this window is that it has high the sensitivity to the outliers in the detection of dFC. To overcome this limitation tapered windows were used in many studies for capturing dFC. The size of the sliding window (tapered window) can be chosen based on the periodic behavior of the time courses. By using these sliding windows, it is possible to evaluate the amount of variability in the resulting FC time series.

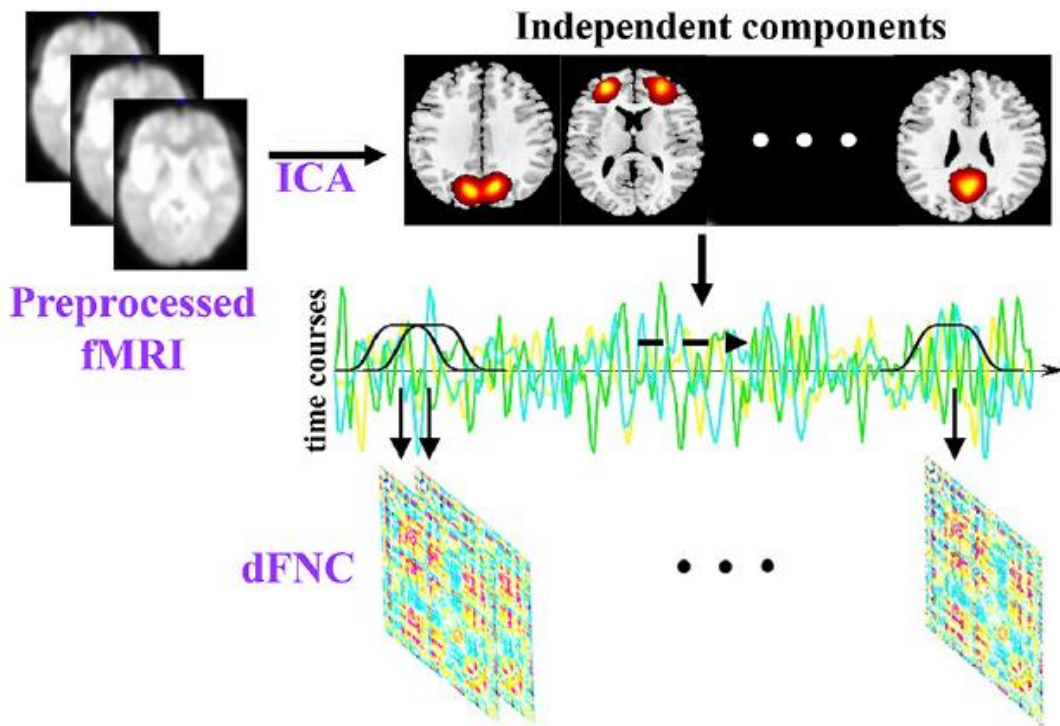


Figure 2.10. Obtaining the functional connectivity matrices by using a sliding window [52].

2.8 K-means Technique

K-means is a well-known technique used for clustering the data [53]. This clustering technique has been used in different fields and applications for separating the data such as image segmentation and market segmentation. In k-means algorithm, K non-overlapping clusters with K centroids are picked and then each sample of the data is assigned to the nearest centroid. The centroids are estimated in such a way to minimize the total error. The error for each sample is defined as a function that measures the distance between a sample and its cluster centroid. The basic k-means algorithm for finding K clusters is applied by following the steps given below,

1. Select K points (samples) as the initial centroids.
2. Assign all the samples to the closest centroid.
3. Recompute the centroid of each cluster.
4. Repeat steps 2 and 3 until the centroids don't change (or change very little).

Even though the k-means is a well-known clustering method and has very simple implementation, it is worth mentioning one of its disadvantages. K-means clustering might not be well-suited for clustering of high dimensional data such as images. It results from the fact that using the distance measures such as Euclidian distance over the high dimensional spaces is not intuitive. For instance, in the case of the high dimensional images, k-means considers the pixel-wise distance for clustering the images that does not correspond to perceptual or semantic distance. Figure 2.11 shows an example that k-means clustering might fail, and the original image and three other images might fall into the different clusters based on their pixel-wise distance while we expect them to be in the same cluster based on their perceptual or semantic similarity.

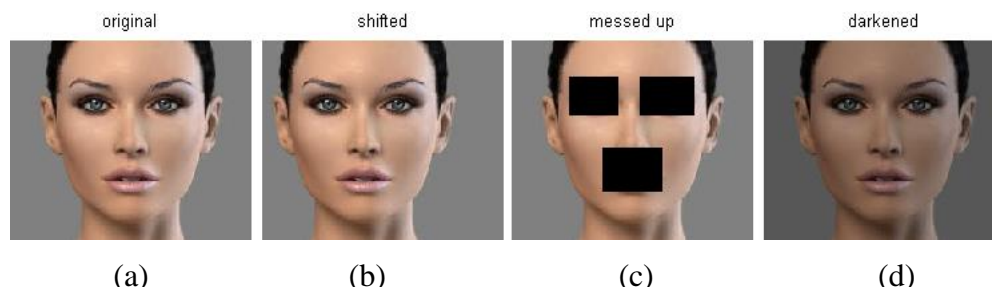


Figure 2.11. K-means clustering fails to put image (b), (c) and (d) in the same cluster as image (a) [54].

2.9 Two Sample T-Test

T-statistics is a statistical method that is employed for comparing the means of two groups and assessing if this two groups are different or not. In other words, this method helps to investigate the degree of difference between two groups and the possibility that this difference could have happened by chance. This degree of difference is obtained based on: 1- The distance between the mean intensities of the two groups and 2- The spread of distribution of each group and the degree of overlap in distributions. As shown in Figure 2.12.

T-value is computed as,

$$t = \frac{\mu_1 - \mu_2}{\sqrt{\frac{s_1^2}{n_1} + \frac{s_2^2}{n_2}}} \quad (2.9)$$

where μ_1 and s_1^2 are the mean and sample variance of group 1, whereas μ_2 and s_2^2 are the mean and sample variance of group 2. Every t-value has a corresponding p-value. The p-value for a t-statistic gives the probability that the difference between two groups happens by chance.

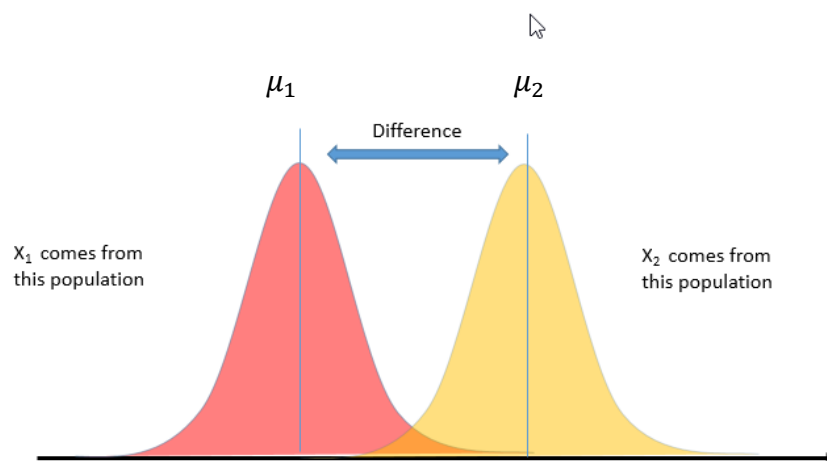


Figure 2.12 Two independent populations [55].

2.10 Summary

The purpose of this chapter was to present some background materials in study of the functional brain connectivity in the resting state fMRI. First, we explained how to preprocess and prepare the fMRI data. Then, group ICA which is an extension of ICA method was introduced. We explained how to use group ICA to capture independent components in this study. Then, we discussed how to choose appropriate components and exclude the artifact components. After that, we explained about functional connectivity matrix and how to capture dynamic functional connectivity using sliding windows. Finally, the two-sample t-test method for obtaining group difference was described.

CHAPTER 3

Group Difference Study Using Convolutional Autoencoder

3.1 Introduction

In this chapter, we study the dynamic functional brain connectivity in fMRI data by using a convolutional autoencoder for obtaining the different connectivity patterns. A brief introduction of artificial neural networks is given in Section 3.2. The convolutional neural networks as a type of neural networks used for 2D data are described in Section 3.3. In Section 3.4, the convolutional autoencoders and their architecture are explained. In Section 3.5, we present the steps carried out to obtain dynamic functional connectivity. First, we apply the group ICA technique on the preprocessed resting-state fMRI data to get the independent components of fMRI data (brain regions) and the corresponding time-courses. A sliding window is then passed through the time-courses and a correlation matrix is obtained for each segment of the time-courses. As our main contribution, we use a convolutional autoencoder for the first time in order to obtain the correlation matrices with the common functional connectivity patterns. By using these connectivity patterns, we are able to study the differences in the functional connectivity in brain regions of the healthy control subjects and that of patients. The Figure 3.1 shows the pipeline for studying the dynamic functional connectivity.

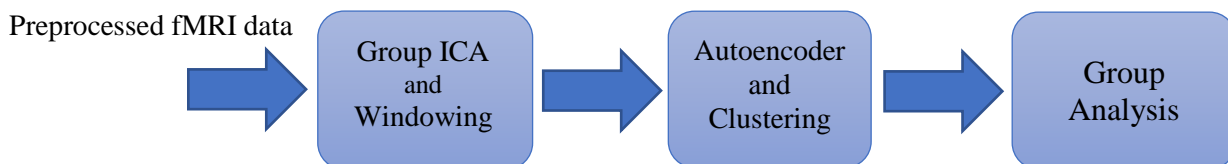


Figure 3.1. The pipeline of dynamic functional brain connectivity study.

3.2 Introduction to Neural Networks

Our brain uses the extremely large interconnected network of neurons for information processing. A neuron, such as the one shown in Figure 3.2, collects inputs from other neurons using dendrites. The neuron sums all the inputs and is fired if the resulting value is greater than a threshold. The signal from the fired neuron is then sent to other connected neurons through the axon.

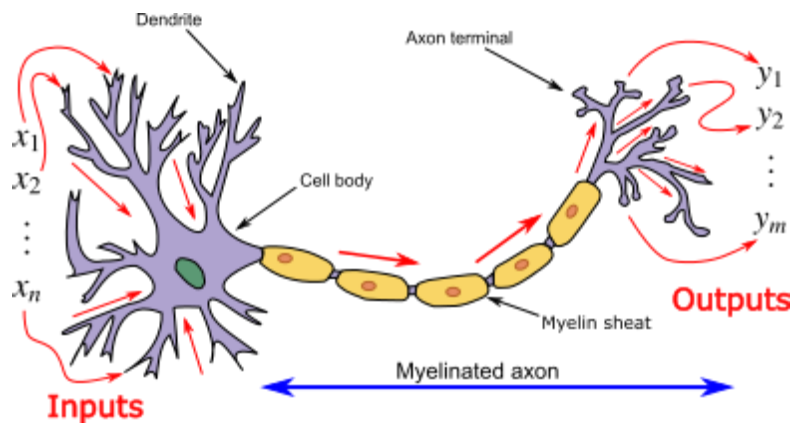


Figure 3.2. The physiological representation of a neuron [57].

Artificial neural network (ANN) is a computing system inspired by the brain neural networks [56]. An artificial neural network is a function ($f: Z \rightarrow O$) that takes each sample from the input data Z and maps it to an output, O . This mapping is carried out by making meaningful connections between a number of neurons. Each neuron in a neural network gets a value determined by a weighted sum of all the inputs followed by an activation function [58] as shown in Figure 3.3. Activation function plays an important role in the artificial neural networks. The activation function decides whether a neuron should be activated or not. So, for each neuron j in the network, its output O_j is defined as:

$$O_j = \phi(\sum_{k=1}^n w_{kj} z_k + b_j) \quad (3.1)$$

where ϕ is the activation function, n is the number of inputs to neuron j , w_{ij} is the weight between neurons i and j , and b is the bias value. The commonly used activation functions in neural networks are Sigmoid, Tanh and ReLU as shown in Figure 3.4.

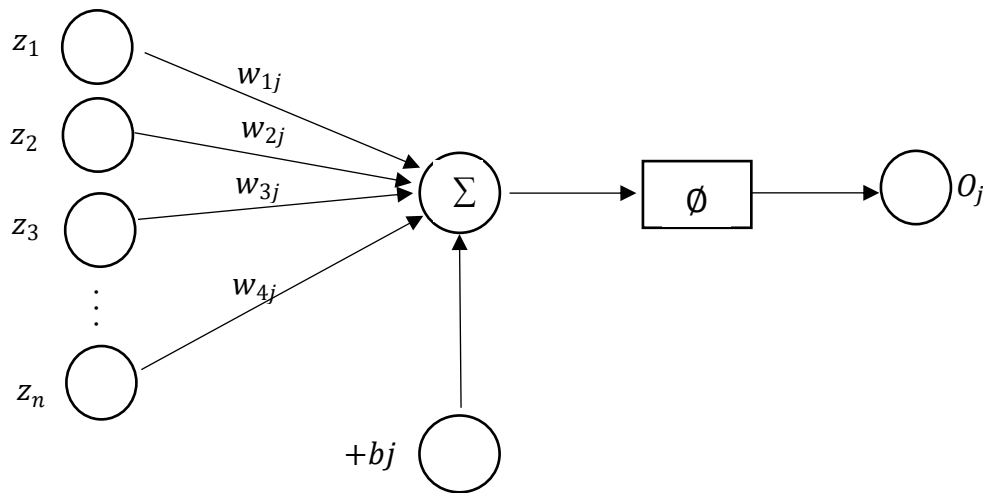


Figure 3.3. The computation in a neuron.

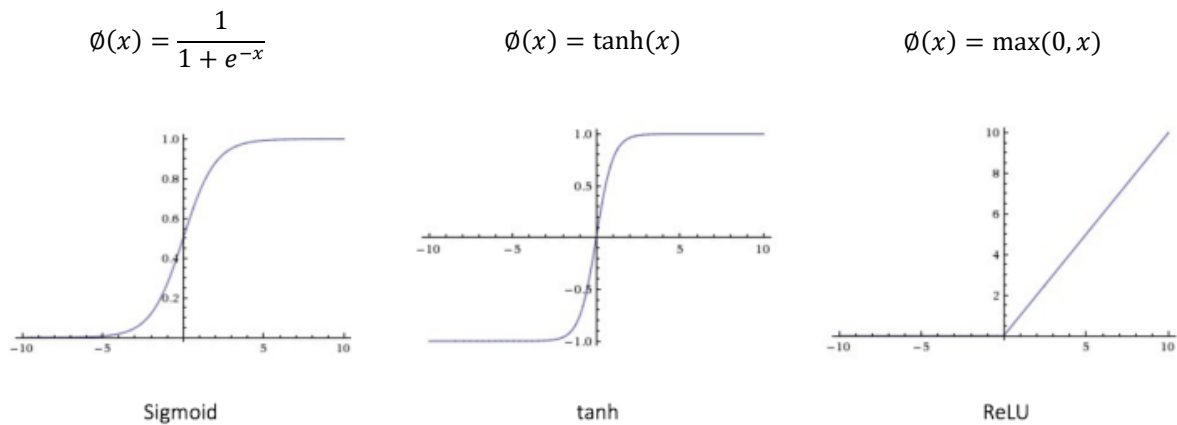


Figure 3.4. The most common activation functions [59].

A neural network consists of a sequence of layers. Each layer uses the output of its previous layer as the input. Figure 3.5 shows a simple multi-layer neural network. Beside input and output layers, other layers of the network are called hidden layers. The input data are processed using the hidden layers and the results are passed to the output layer. In fact, the neural network maps the input data in the first layer to a set of prediction scores in the output layers using a set of weights in each layer. A cost function is defined to quantify the agreement between the prediction scores at output layer and the expected output (ground truth labels). Mean square error and cross entropy cost function are the most popular cost functions used in the neural networks. The weights of the neural network should be adjusted during training in such a way that minimize this cost function. In order to minimize the cost function, the weights in the neural network are optimized using a method called backpropagation. Backpropagation is a method used for training a neural network by calculating a gradient that is needed for updating the network weights. This process is carried out by computing the error at the output and distributing it backwards throughout the network layers. During the backpropagation, each weight of the network is updated using the gradient descent as given by,

$$w_{ij} = w_{ij} - \alpha \frac{\partial J}{\partial w_{ij}} \quad (3.2)$$

where w_{ij} is the weight between neurons i and j , J is the cost function of the neural network and α is the learning rate used for updating the weight. In fact, the gradient descent is a way to minimize the cost function J parameterized by the model weights by updating the weights in the opposite direction of the gradient of the cost function with respect to the weights. The learning rate α determines the size of the steps that is taken in the gradient descent direction to reach to the local minimum of cost function. Stochastic gradient descent (SGD) is a variation of gradient descent

that estimates the gradient from a small number of samples chosen randomly from training data in each iteration (minibatches). SGD converges much faster than the original gradient descent in which all the data in the training set are used for estimation of the gradient in each iteration. Hence, SGD is used more often for training the neural network.

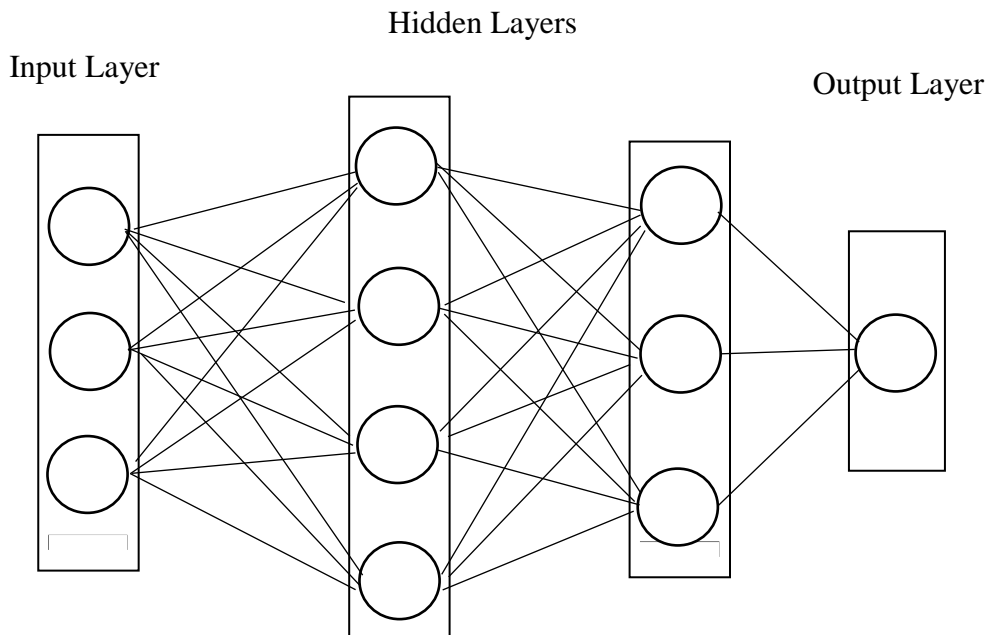


Figure 3.5. A typical structure of a multi-layer neural network.

3.3 Convolutional Neural Networks

Convolutional neural network (CNN) is a type of neural networks that is typically used for 2D data such as images. The architecture of a Convolutional neural network is inspired by the organization of the Visual Cortex in which the individual neurons respond to stimuli in a restricted region of the visual field known as the receptive field. The convolutional neural network takes advantage of spatial structures in the input data by convolving a kernel to the input data to detect local features

of the input [59]. Since the same kernel with the same parameters is used on every unit of the input data (parameter sharing), the number of parameters required to train a neural network drastically decreases. The convolutional neural network learns the feature representations of the input in each layer in a hierarchy by obtaining the low-level features in first layers and high-level features in the last layers. A typical convolutional neural network is shown in Figure 3.6. A convolutional neural network consists of two main building blocks called convolutional layers and pooling layers.

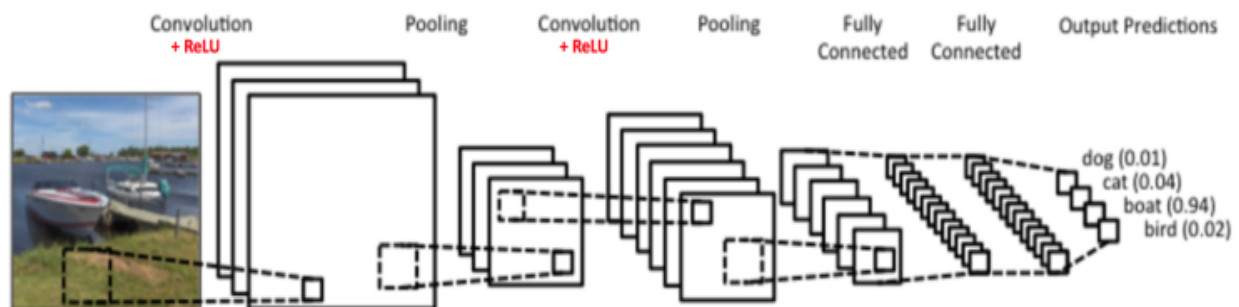


Figure 3.6. A typical architecture of a convolutional neural network [60].

3.3.1 Convolutional Layer

The convolutional layer is the main building block of a convolutional neural network. In a convolutional layer, the convolution is performed by sliding a kernel over the input and carrying out a matrix multiplication and summation. A set of kernels is used in each convolutional layer to extract different kinds of features from the input data [61] and generate the layer output, called feature map. Stride and zero-padding are two important properties of each convolutional layer.

- **Stride:** Stride is the number of steps by which we slide the kernel over the input image. When the stride is 1 then we move the kernels by one step at a time. Using a larger stride leads to have smaller feature maps at the output of the layer.

- **Zero-Padding:** The spatial size of the feature map gets smaller than input size after performing the convolution on the input. In order to prevent the feature map from shrinking, zero-padding is applied to input image by adding zero-value pixels around the input image as shown in Figure 3.7. The size of a convolution layer output (feature map) would be the same as that of the input if we employ zero padding with the size of:

$$p = \left(\frac{f - 1}{2}\right) \quad (3.3)$$

where f is the width of the kernel used in the convolutional layer

The depth of the output volume (feature map) in each convolutional layer is determined by the number of kernels used in that layer. Also, the spatial size of output can be calculated by having input size, width of the kernel, the number of padding and stride. If we convolve the kernels with width f to a $P \times P$ image with padding of p and stride of q , the spatial size of the output (feature map) is determined by,

$$Output\ size = \frac{P + 2p - f}{q} + 1 \quad (3.4)$$

0	0	0	0	0	0
0	4	8	30	23	0
0	13	25	2	16	0
0	36	3	1	7	0
0	9	17	12	3	0
0	0	0	0	0	0

Figure 3.7. An example of zero padding operation.

The rectified linear unit (RELU) is the most commonly used activation function in convolutional neural network that is placed after convolutional layers to introduce the non-linearity to the feature maps.

3.3.2 Pooling Layer

Pooling layer is often used in CNNs to reduce the spatial size of the input and feature maps. This reduction in the size is carried out by breaking the input into different non-overlapping regions. Each region is then replaced by a single value. It results in decreasing the size of the layer output (feature map) while preserving the most important information contained within each region [62]. The operation that is performed on each region determines the type of the pooling layer. This operation can be an average operation within each region, selecting the maximum value in each region or any other types of operation. Selecting the maximum value is the most common type of pooling operation. In that case, the layer is called max-pooling layer. The advantage of max-pooling layer is that extracted features would be the same even with a small shift of the input data. An example of max-pooling operation is illustrated in Figure 3.8.

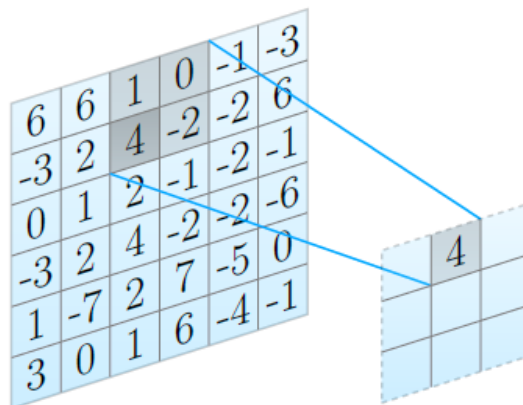


Figure 3.8. Max pooling operation [63].

A convolutional neural network consists of a sequence of convolutional and pooling layers. In supervised learning applications such as classification, some fully connected layers are usually added after the last layer of CNN followed by an output layer for classification. A cost function is defined to quantify the agreement between the given label for each input of the convolutional neural network and the score obtained in the output layer. Backpropagation algorithm is used to update all the weights of the network in order to minimize the cost function [61]. In other words, the weights of the network are updated in such a way to make the output in agreement to the ground truth label. Convolutional neural network can also be used for unsupervised learning. In this case, it is not required to have any labels for training. One of convolutional neural networks used for unsupervised learning is called convolutional autoencoder.

3.4 Convolutional Autoencoders

A convolutional autoencoder is a type of convolutional neural networks that is used for unsupervised learning. The convolutional autoencoder is based on an encoder-decoder paradigm as shown in Figure 3.9. The encoder of autoencoder consists of several convolutional and pooling layers that transforms an input image and produces a low-dimensional representation of the image. This low-dimensional representation of the input is also referred to latent representation of the input. The decoder of autoencoder consists of deconvolutional layers or up-sampling layers followed by convolutional layers. The decoder is responsible to reproduce the input at the output by using the latent representation of the input. In other words, the encoder compresses the input data and the decoder reconstructs the input from the compressed data.

A convolutional autoencoder is trained end-to-end in an unsupervised way by using the input data as the label. The training is carried out through the minimization of the mean squared error (MSE) cost function given by,

$$J = \min_{w,U} \frac{1}{n} \sum_{i=1}^n \|g_u(f_w(x_i)) - x_i\|_2^2 \quad (3.5)$$

where $f_w(.)$ is the output of the encoder (latent representations) and w is the set of weights used in the encoder. Also, $g_u(.)$ is the output of decoder and u is all the weights in the decoder. The weights of the autoencoder (w and u) are updated during the training using the backpropagation and gradient descent in order to minimize the cost given in Equation 3.5. After the training, the autoencoder learns to reconstruct the input at the output.

The autoencoders can be employed in different tasks such as feature extraction, dimensionality reduction, and clustering.

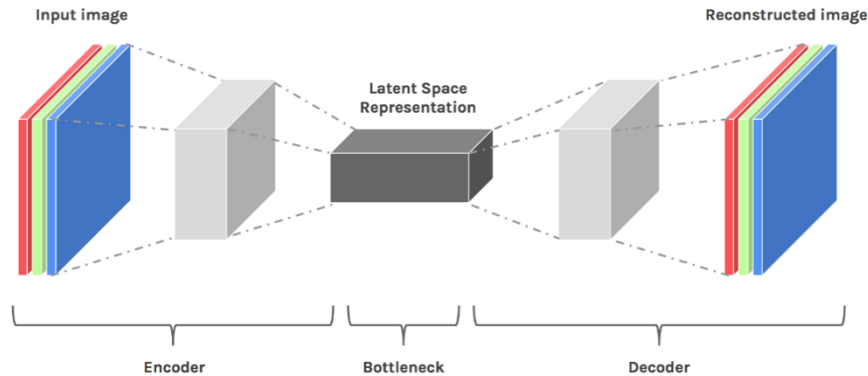


Figure 3.9. The general architecture of a convolutional autoencoder [64].

3.5 The Pipeline of Dynamic Functional Brain Connectivity Study

In this section, we present the pipeline for the capturing dynamic functional brain connectivity in the resting-state fMRI data along with the convolutional autoencoder as the novel method for obtaining of the FC patterns.

3.5.1 Group ICA and Windowing

As explained in Section 2.5, the group ICA is applied to the preprocessed fMRI data of all the subjects to obtain the independent components and the corresponding time-courses. A sliding window is then moved on the time-courses of each subject to obtain a different correlation matrix for each slice of time courses as shown in Figure 2.10. Hence, $D \times M$ number of correlation metrics are generated, where D is the number of sliding windows for each subject and M is the number of subjects. Dynamic functional connectivity can be summarized into a finite number of functional connectivity patterns usually referred to as “functional connectivity states”. In order to capture the functional connectivity states, all the correlation metrics should be clustered. The clustering of high dimensional data has some limitations. When the number of dimensions is high, the distance between any two points in the dataset converges. It means the maximum distance and minimum distance between any two points of dataset will be close. To solve the problem of clustering of high dimensional data, convolutional autoencoder is used to capture connectivity states.

3.5.2 Convolutional Autoencoder for Obtaining FC States

The convolutional autoencoder explained in Section 3.4 is used for the first time for obtaining the connectivity states as the main contribution of this thesis. After designing a convolutional

autoencoder, all the $D \times M$ correlation matrices obtained in the previous section are used as an input to the autoencoder. First, the autoencoder needs to be trained using these correlation matrices. During training of the convolutional autoencoder, all the weights in the kernels are updated in such a way that the reconstruction error (defined by MSE) between the reconstructed connectivity matrices at the output of autoencoder and the original connectivity matrices in the input is minimized. The update of the weights is carried during training by using stochastic gradient descent (SGD) and backpropagation. The training procedure continues until there is no sensible reduction in reconstruction error. After training the convolutional autoencoder is finished, the correlation matrices are passed through the encoder of convolutional autoencoder one by one and the output of the encoder (output of the middle layer of autoencoder), known as the latent representation of the input is extracted.

Instead of clustering correlation matrices directly, we cluster their corresponding latent representation obtained at the middle layer of autoencoder. Each cluster represent a state of connectivity for dynamic functional connectivity analysis. All the correlation matrices that correspond to the latent representations in a cluster are then considered to have the same pattern and belong to the same connectivity state. Hence, if there are K clusters, each correlation matrix is assigned to one of the K states.

We use a k-means algorithm to cluster the latent representations of the obtained connectivity matrices at the middle layer of the autoencoder and partition them into a set of separate clusters. The optimal number of centroid states is estimated using the elbow criterion, defined as the ratio of within the cluster distances to the between the cluster distances. A search window of K from 2 to 9 was used to obtain the best cluster number.

3.5.3 Group Analysis

After clustering all the functional connectivity matrices by using their latent representations, the median of the connectivity matrices with the similar pattern (with the same cluster ID) is calculated for both healthy subjects and patients. A two-sample t-test is then performed on each cluster in order to determine each pair of the brain regions in the group of the healthy control subjects for which the correlation value is significantly different from that of the corresponding pair of the regions in the group of patients.

The duration of a functional connectivity matrix to remain in one state before switching to another state is referred as dwell time. In order to distinguish the FC in the healthy people from that in the people affected by mental disorders, the average dwell time for each group in each state is computed and compared.

3.6 Summary

In this chapter, a convolutional autoencoder as a novel method for clustering the connectivity matrices was proposed. First, we introduced the neural networks. Then, convolutional neural networks as a type of neural networks and their advantages over typical neural network were presented. Next, a convolutional autoencoder that is a type of CNNs for unsupervised learning was explained. In the last part of this chapter, three main steps of the pipeline used in this study for obtaining the dynamic functional connectivity in the resting-state fMRI data was presented. As the main contribution of this study, a convolutional autoencoder is used to obtain different functional connectivity patterns. For this purpose, after training the convolutional autoencoder by using all the correlation matrices, the latent representations of the correlation matrices are obtained at the output of encoder (middle layer of the convolutional autoencoder). K-means algorithm is then

applied to the latent representations to partition them into a set of separate clusters. Finally, a two-sample t-test is applied on each cluster in order to determine each pair of the brain regions in the group of the healthy control subjects for which the functional connectivity is significantly different from that of the corresponding pair of the regions in the group of patients.

CHAPTER 4: Results and Discussions

4.1 Introduction

In this chapter, the dynamic functional brain connectivity for a group of healthy subjects and a group of patients affected by schizophrenia is studied by using the proposed method for obtaining the connectivity patterns from fMRI data. First, a brief description about the schizophrenia mental disorder is given. The scanner parameters used for the acquisition of fMRI data from healthy subjects and schizophrenia patients are provided. Then, different steps of the preprocessing applied to the raw fMRI data of all subjects are presented. The results for each step of the procedure carried out for obtaining the dynamic functional connectivity, including the group ICA, component selection, windowing and finding the connectivity matrices are explained. Then, the proposed method based on the convolutional autoencoder is used to find the different functional connectivity patterns from the connectivity matrices. In order to demonstrate the effectiveness of using the convolutional autoencoder, some synthetic connectivity matrices are generated. It is shown that the proposed method based on the convolutional autoencoder is able to cluster the connectivity matrices with the same patterns more accurately in comparison to the traditional k-means clustering method. The proposed method is then used to cluster the real connectivity matrices in order to obtain the different functional connectivity patterns. A two-sample t-test is then performed on each functional connectivity pattern in order to determine the pairs of brain regions in the group of healthy subjects in which the functional connectivity is significantly different from those in the group of schizophrenia patients.

4.2 What Is Schizophrenia?

Schizophrenia is a severe mental disorder that occurs in 1 percentage of the world population. This disease is usually characterized by losing the ability to understand the reality (hear voices or see things that are not real), having problem with social interaction, sleeping problem, and difficulty in memorizing. Schizophrenia is thought to be related to a combination of genetic and environmental factors, although the exact cause is not yet known. Unfortunately, there is no clinical test for schizophrenia, and the diagnosis is based on self-reported questionnaires and abnormalities in behavior [65].

4.3 fMRI Data Analysis

In this study, the resting-state data come from the Center for Biomedical Research Excellence (COBRE) [66]. 72 patients with schizophrenia and 74 healthy controls are studied from the released data set. None of the subjects had a history of neurological disorder, mental deficiency, sever head trauma with more than five minutes loss of consciousness and history of drug abuse or drug dependence during the last 12 months before the test. A demographic representation of the COBRE data is shown in Table 4.1.

Table 4.1. Summary of subject demographics.

	Healthy	Patients
Number of subjects	74	72
Age	35.5(18-65)	38.1(18-65)
Gender (M/F)	51/23	58/14

The resting-state fMRI was captured with a single shot echo-planar imaging (EPI). The fMRI scanner parameters that were used for acquisition of the fMRI data are as follows,

TR: 2 s

TE: 29 ms

FOV: 256 mm × 256 mm

Number of slices: 33 slices

Voxel size: 3 × 3 × 4 mm³

Total scan time: 5 minutes (150 TR)

It should be noted that the resting-state fMRI data, anatomical MRI (structural data) and phenotypic features (gender, age, handedness and diagnostic information) are available for every subject.

Pre-processing of fMRI data is carried out using the Statistical Parametric Mapping software (SPM12) [67] implemented in MATLAB. Several steps of preprocessing are applied to the fMRI data as follow,

- Discarding the first 5 image volumes from the fMRI data of each subject to avoid T1 equilibration effect.
- Slice timing correction: The slice timing correction is carried to address the problem of time difference between the slices in a scan of the brain. Since each scan of our fMRI data contains 33 slices, 17th slice (the middle slice) is used as the reference slice for time-slicing correction.

- **Realignment:** For overcoming the head-motion problem that happens during fMRI data acquisition, all the fMRI slices are required to be aligned. For the realignment, 6 parameters are estimated, three parameters for translation and 3 parameters for rotation. Hence, by applying this transformation to fMRI data, all the slices in a scan of fMRI data are aligned to the first image.
- **Coregistration:** Coregistration is carried out to align the functional MRI images of each subject to the structural data (MRI data).
- **Spatial normalization:** Prior to carrying out any group analysis, it is required to normalize the fMRI data of each subject and transform them into the same space. For this purpose, we use MNI (Montreal Neurological Institute) template.
- **Smoothing:** A spatial Gaussian smoothing with a kernel size of $6 \times 6 \times 6 \text{ mm}^3$ is applied to the normalized fMRI data for removing the noise and artifact.

After applying the preprocessing steps, group ICA is carried out by using the GIFT toolbox [68]. In the group ICA method, a set of independent components are estimated from the fMRI data of a group of subjects. Prior to applying the group ICA to the fMRI data, two levels of data-reduction are carried out to reduce the computational burden. These two data reduction steps are done by using the principal component analysis (PCA) method. The first data reduction step is done to reduce the dimension of the data for each individual subject (subject-level PCA), resulting in estimating 120 principle components for each subject. After reducing the dimension of the fMRI data for each subject, the dimensionally-reduced fMRI data of all the subjects are vertically concatenated into a single matrix. Then, another data reduction step is applied to this concatenated matrix (group-level PCA) to estimate 100 principle components at the group level. In order to

make these 100 principle components maximally independent, an ICA transform based on the infomax algorithm is applied to these principle components to obtain 100 independent components (ICs) for the fMRI data. ICA algorithm can give different independent components when run multiple times, this may happen from the fact that these algorithms may converge to a local minimum. Hence, the stabilization of ICA results is guaranteed by using ICASSO [69] in which ICA algorithm is run for several times. Thus, we have run the ICA algorithm for 10 times and combined the results from several runs of the ICA algorithm and obtained a set of independent components that is more accurate than any of the independent component sets provided by a single run of ICA. After obtaining 100 independent components using the group ICA, we need to explore and select only a subset of them by considering several aspects and properties as follows,

- 1) The location of component: In order to check the location of the components, MRIcron software [70] is used. This software is an image viewer for neuroimaging data and is able to show the region of interest. By using this software, we make sure that the peak of each component obtained by the group ICA is located in the grey matter (GM) area of the brain and also the components are not ring-shaped resulted from head motion. In other words, the ring-shaped components and the components located in the white matter (WM), cerebrospinal fluid (CSF) or those having overlap with the brain arteries should be excluded from the set of independent components in our study. For example, Figure 4.2 shows a ring-shaped component removed from the set of independent components.

- 2) The frequency spectrum of the time courses: The power spectral of the time-courses corresponding to the estimated independent components should exhibit the low frequency power with presence of the highest power between 0.01- 0.1 Hz. Figures 4.3 shows a

component that is excluded from the set of components since its corresponding time-course has high frequencies.

Hence, after exploring all the 100 independent components, 52 ICs have been selected based on the location of the components and spectral characteristic of their corresponding time-courses. The appropriate components are then grouped into seven networks based on their anatomical location and functions. These seven networks are called subcortical (SC), auditory (AU), visual (VIS), sensorimotor (SM), cognitive control (CC), default mode (DM), and cerebellar (CB) networks as described by Allen *et al* [8].

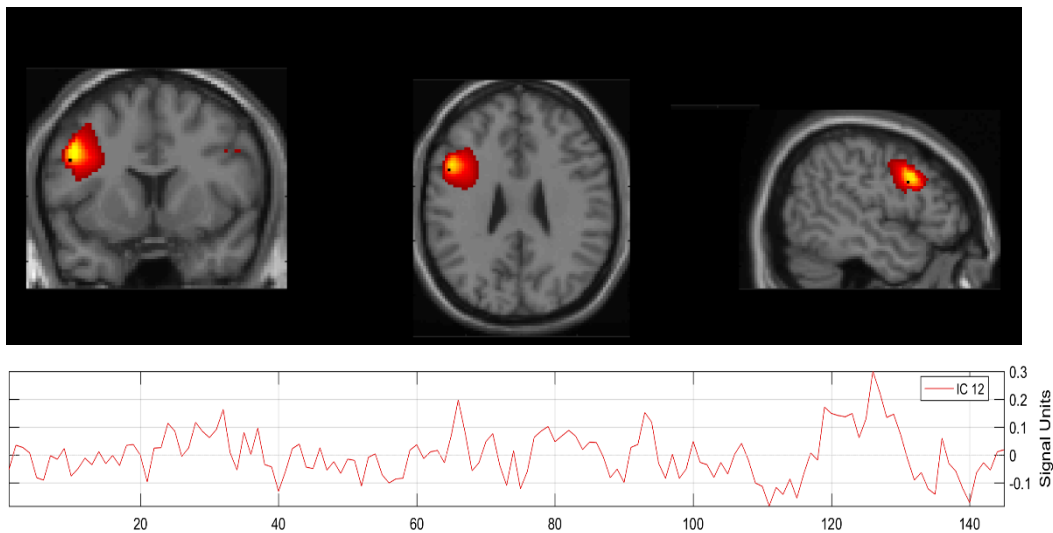


Figure 4.1. An independent component (IC) and the corresponding time-course.

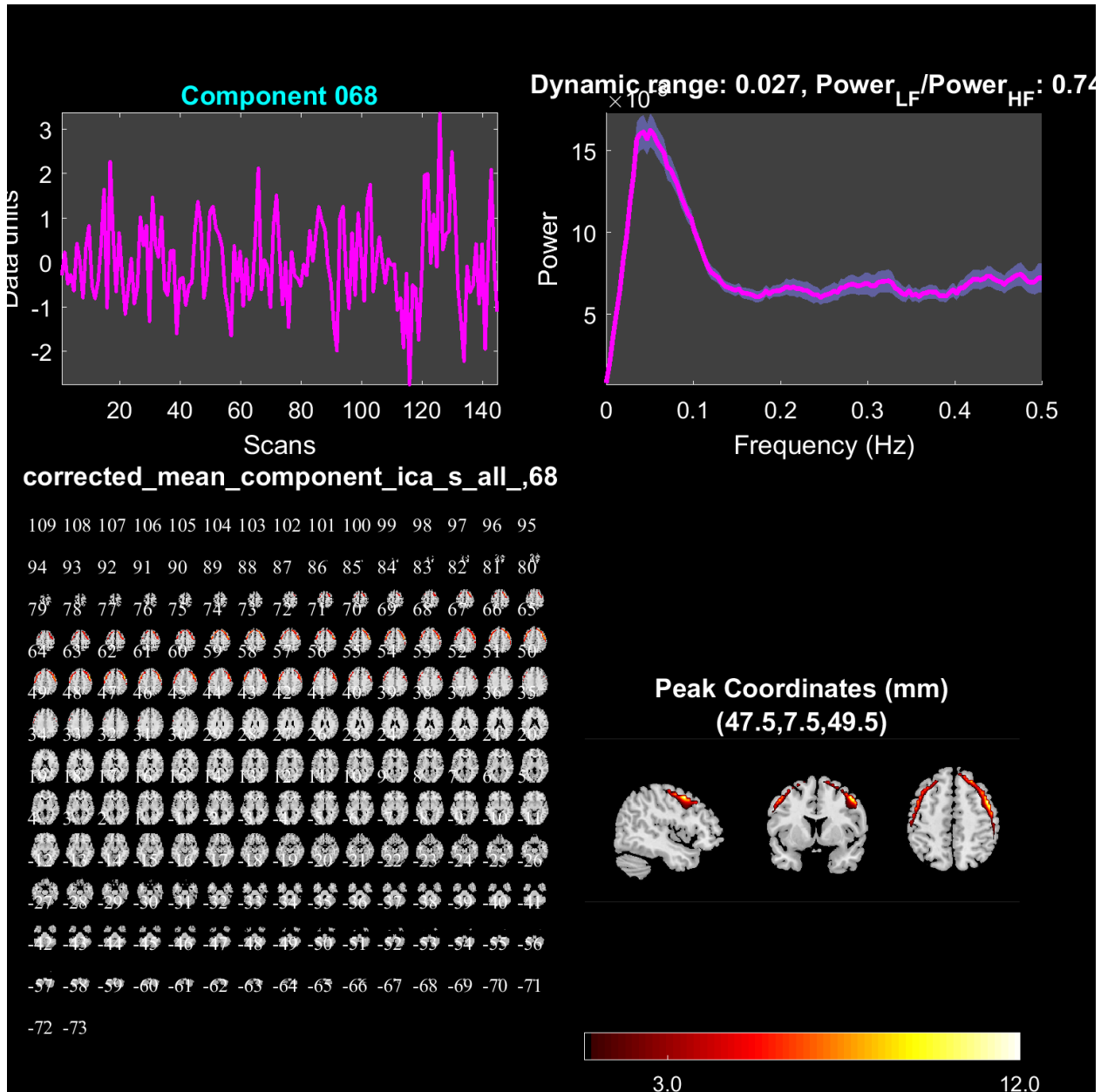


Figure 4.2. The output of GIFT software showing an independent component, its corresponding time-course and frequency spectra.

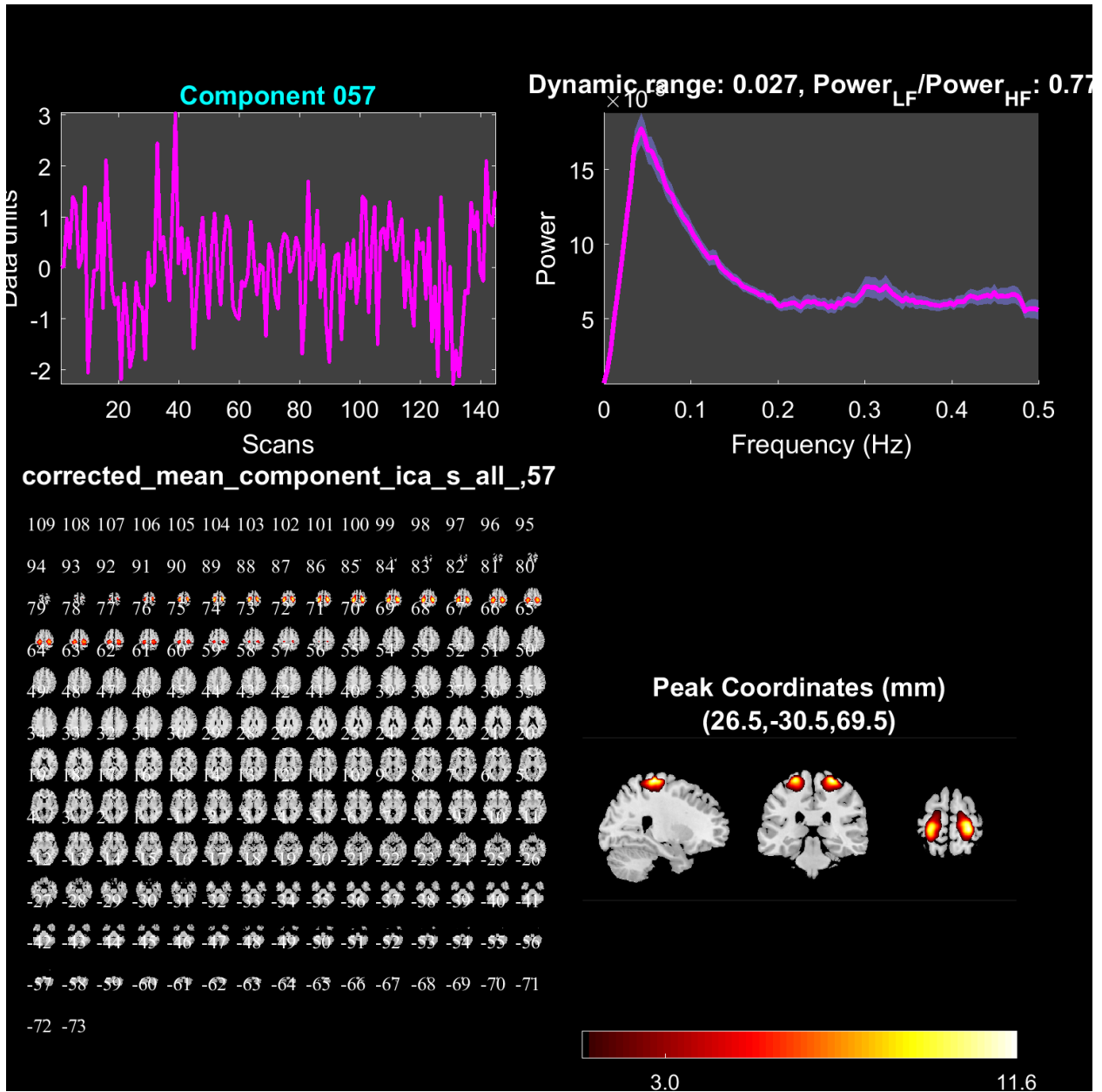


Figure 4.3. The output of GIFT software showing an independent component, its corresponding time-course and frequency spectra.

Then, a tapered window is passed through the time-courses corresponding to the 52 selected components by the step of 1TR (2 sec). This tapered window is created by using a rectangle with width = $30 \times \text{TRs} = 60$ s convolved to a Gaussian filter with the standard deviation of $3 \times \text{TRs}$. The 52×52 connectivity matrix is computed within each segment of the time-courses enclosed inside the sliding window. Since the length of the time-courses and window size are $145 \times \text{TR}$ and $30 \times \text{TR}$, respectively, 115 connectivity matrices are obtained for each subject. Hence, we get a total of $115 \times 146 = 16590$ correlation matrices for all the subjects. It should be noted that for obtaining a meaningful connectivity matrix in each window, we estimate the correlation matrix from the regularized precision matrix to overcome the problem of information insufficiency in short-time segment in each window [71]. Also, all the correlation matrices are fisher transformed ($z = \arctanh(r)$) for variance stabilization.

In order to obtain different functional connectivity patterns occurring over time, all the connectivity matrices need to be clustered. For this task, we design a 7- layer convolutional autoencoder that consists of an encoder and a decoder, as shown in Figure 4.4. The encoder of autoencoder consists of 4 convolutional layers and 3 pooling layers that reduces the spatial dimension of the 2D input to obtain its latent representation. The decoder of autoencoder consists of 3 up-sampling, each followed by a convolutional layer. The decoder is responsible to reconstruct the 2D input at the output of autoencoder from the latent representation (encoder output). The 3×3 convolutional kernels with stride of 1 (q:1) are used in each convolutional layer of autoencoder. A Relu activation function is used after each convolutional layer to obtain the output of each layer (feature map). Also, a 2×2 max pooling with stride of 2 (q:2) is used in each layer of encoder to reduce the spatial dimension of the feature maps by half. The properties of different layers of the designed autoencoder are given in Table 4.2.

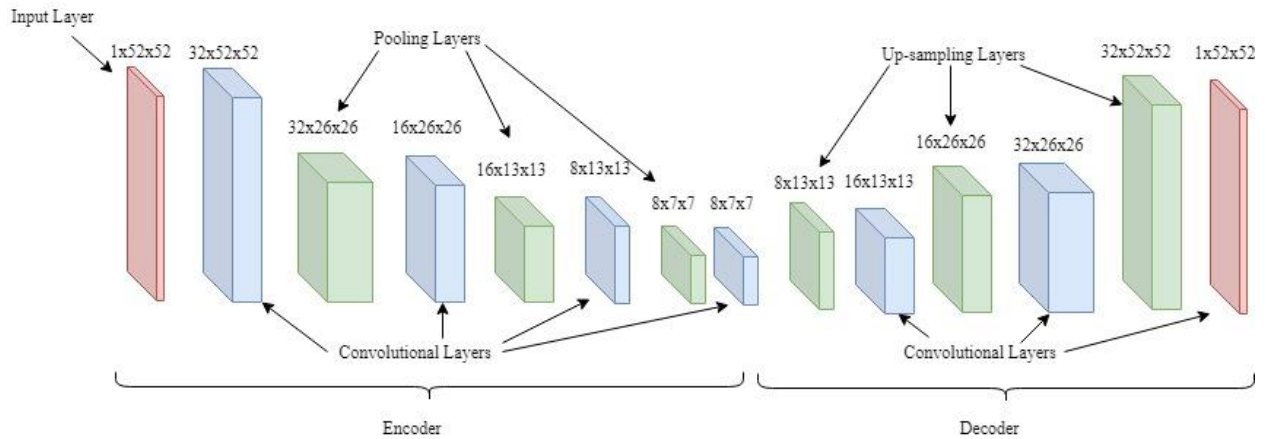


Figure 4.4. The architecture of the designed convolutional autoencoder for obtaining functional connectivity patterns.

All of the 16590 connectivity matrices obtained in the previous step are turned into 2D grayscale images. These images are then used for the training of the convolutional autoencoder.

The convolutional autoencoder is trained on a NVIDIA GTX-1070 GPU using TensorFlow. For the training, a stochastic gradient descent (SGD) optimizer with initial learning rate 0.005 and the batch size of 32 are used. The loss is defined as the square difference between input image and the decoded image at the output of the autoencoder network. Figure 4.5 shows that the loss gradually decreases during the training of the autoencoder.

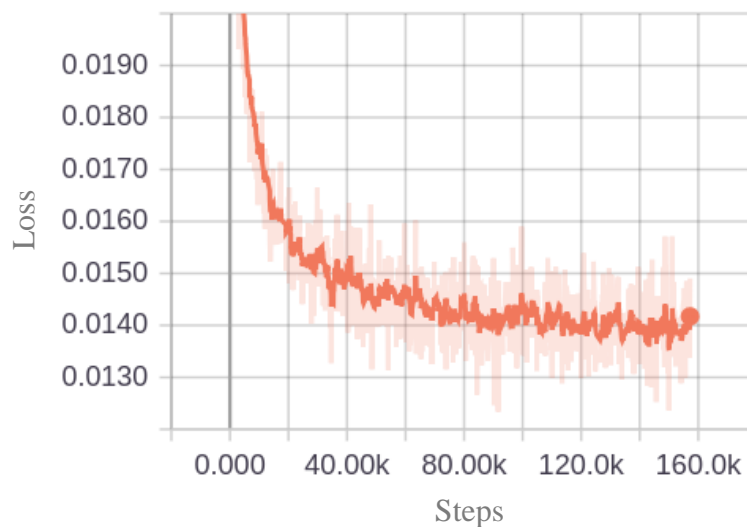


Figure 4.5. Loss curve for the convolutional autoencoder during the training.

Table 4.2. Convolutional autoencoder layers.

Autoencoder layers	Kernel size	stride	Input size	Output size
Conv layer	3x3	q:1	1x52x52	32x52x52
Pooling layer	2x2	q:2	32x52x52	32x26x26
Conv layer	3x3	q:1	32x26x26	16x26x26
Pooling layer	2x2	q:2	16x26x26	16x13x13
Conv layer	3x3	q:1	16x13x13	8x13x13
Pooling layer	2x2	q:2	8x13x13	8x7x7
Conv Layer	3x3	q:1	8x7x7	8x7x7
Up-sample	–	–	8x7x7	8x13x13
Conv Layer	3x3	q:1	8x13x13	16x13x13
Up-sample	–	–	16x13x13	16x26x26
Conv Layer	3x3	q:1	16x26x26	32x26x26
Up-sample	–	–	32x26x26	32x52x52
Conv Layer	3x3	q:1	32x52x52	1x52x52

After training the convolutional autoencoder using the 16590 sample for 160000 steps, the outputs of encoder in the autoencoder (Latent representations) with the size of $8 \times 7 \times 7$ are obtained for all of these 16590 samples. Hence, 16590 latent representations, each correspond to one of 16590

original 52×52 correlation matrices are obtained. Then, these latent representations are clustered using the k-means method.

There are no ground truths for the evaluation of the proposed method performance for clustering the connectivity matrices. Hence, in order to show the superiority of the proposed method for clustering the connectivity matrices over that of k-means, 16000 matrices with the same size as the connectivity matrices (52×52) and four different patterns are generated (4000 matrices for each pattern). These matrices can be considered as the synthetic connectivity matrices. Figure 4.6 shows one sample of the generated 52×52 matrices presented by greyscale image for each of the four patterns.

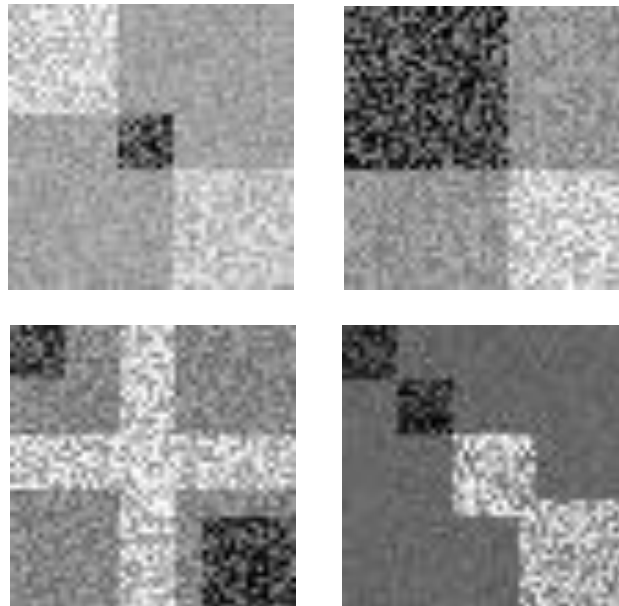


Figure 4.6. One sample of synthetic connectivity matrices from each pattern.

These 16000 generated matrices are turned into grayscale images and are then passed one by one through the encoder part of the convolutional autoencoder trained by the real connectivity matrices. Hence, 16000 latent representations of the input matrices (synthetic connectivity matrices) are obtained at the output of the encoder. Finally, the k-means is applied to these 16000 latent representations to cluster them.

T-distributed Stochastic Neighbor Embedding (t-SNE) is a nonlinear dimensionality reduction technique that is suitable for embedding high-dimensional data in a low-dimensional space (two or three dimensions) for visualization. T-SNE models each high-dimensional data by a two- dimensional or three-dimensional point in such a way that similar objects are modeled by nearby points and dissimilar objects are modeled by distant points. In Figures 4.7 and 4.8, t-SNE is used for the 2D visualization of the synthetic connectivity matrices and their corresponding latent representations obtained by the designed convolutional autoencoder, respectively. Four different colors are used to distinguish the samples with different patterns.

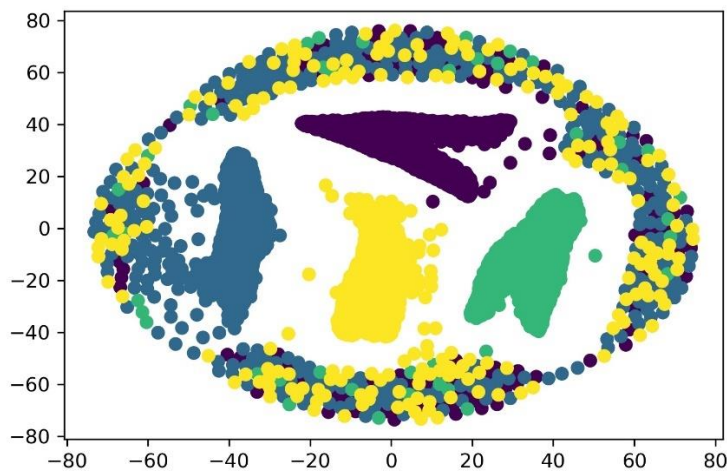


Figure 4.7. Visualization of the synthetic connectivity matrices using t-SNE.

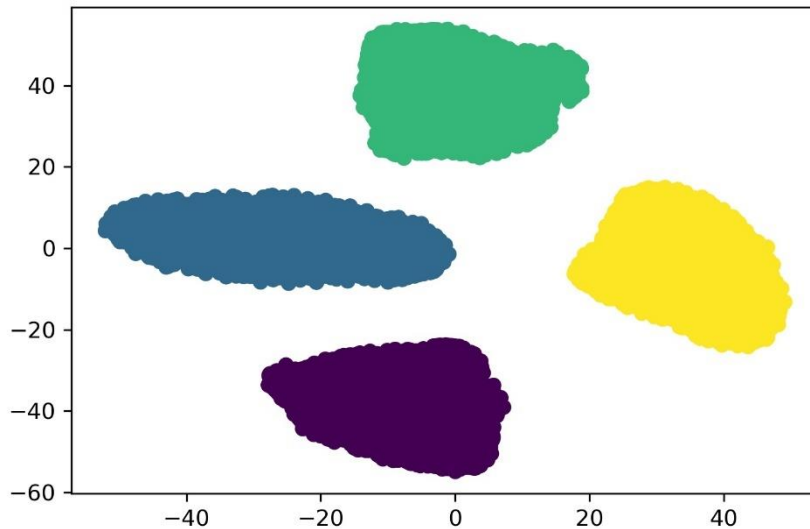


Figure 4.8. T-SNE visualization of the latent representations of the generated connectivity matrices obtained by the designed CAE.

Figure 4.7 shows that t-SNE is unable to separate the high dimensional synthetic connectivity matrices with the same pattern from those with other patterns. However, it is observed from t-SNE in Figure 4.8 that the latent representations of the synthetic connectivity matrices with the same pattern are grouped together and are far from those with other patterns. Hence, it is expected that clustering the latent representations of the connectivity matrices obtained by the designed autoencoder is more precise than clustering of connectivity matrices directly. Table 4.3 shows the result of k-means applied directly to the synthetic connectivity matrices. It also shows the results of k-means applied to the latent representations of connectivity matrices obtained by the designed convolutional autoencoder (CAE). The values in the table show the number of samples (out of 16000) in each cluster and the percentage of error.

Table 4.3. Number of matrices in different clusters.

	Cluster 1	Cluster 2	Cluster 3	Cluster 4	Error
K-means	3951	4295	3754	4000	3.7%
CAE +k-means	4000	4000	4000	4000	0

The results in Table 4.3 shows that the performance of the proposed clustering method in which the k-means is applied to the latent representations obtained by autoencoder is much better than that of k-means directly applied to the generated connectivity matrices.

Now, in order to capture the reoccurring FC patterns in fMRI data, we use the proposed method by applying the k-means to the latent representations of 16590 correlation matrices obtained by the designed autoencoder (output of the middle layer of autoencoder). The ‘elbow’ criterion is used to select the optimum number of clusters for the latent representations. By changing the number of clusters in a search window from 2 to 9, an elbow is observed when the number of clusters is 4. Hence, the number of clusters that is the number functional connectivity patterns (states) is considered to be 4 in our study. The averages of the correlation matrices corresponding to all the latent representations with the same cluster id (state) are shown in Figure 4.9. Figures 4.10 and 4.11 show the group-specific medians for each state of schizophrenia subjects and healthy subjects, respectively.

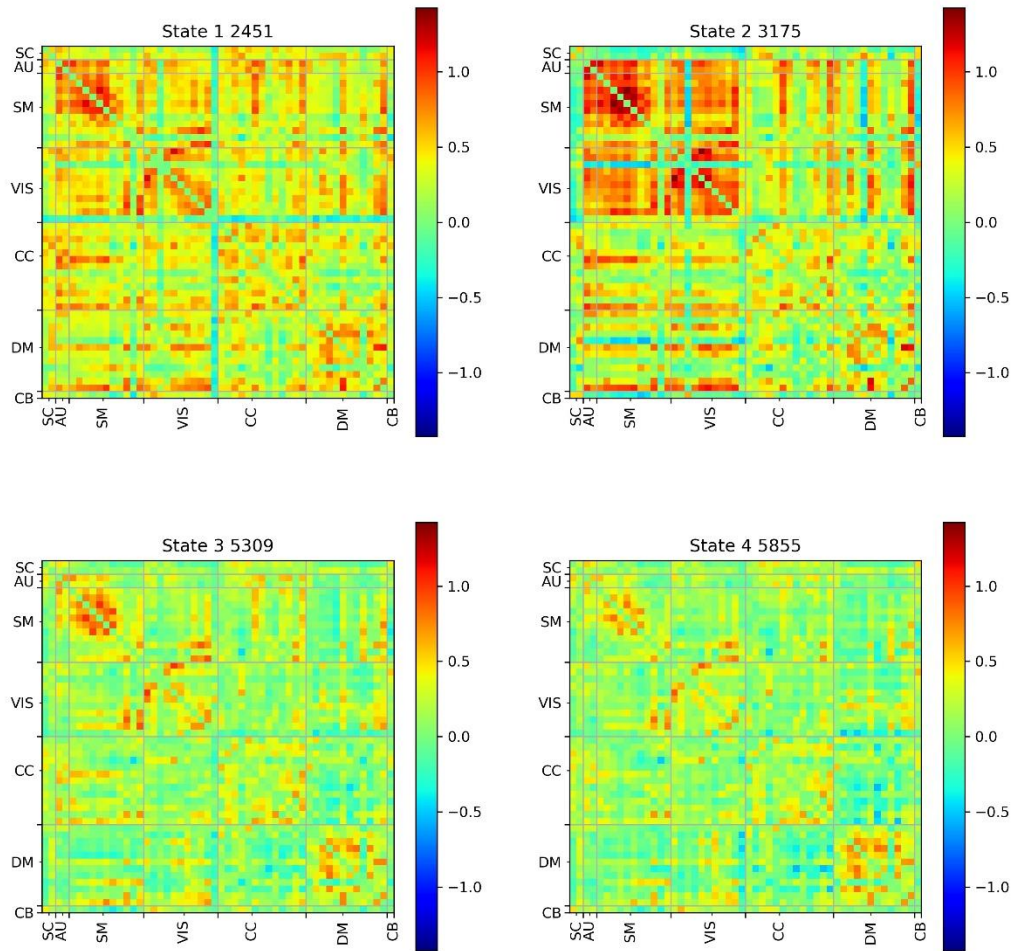


Figure 4.9. Average of the correlation matrices in each state.

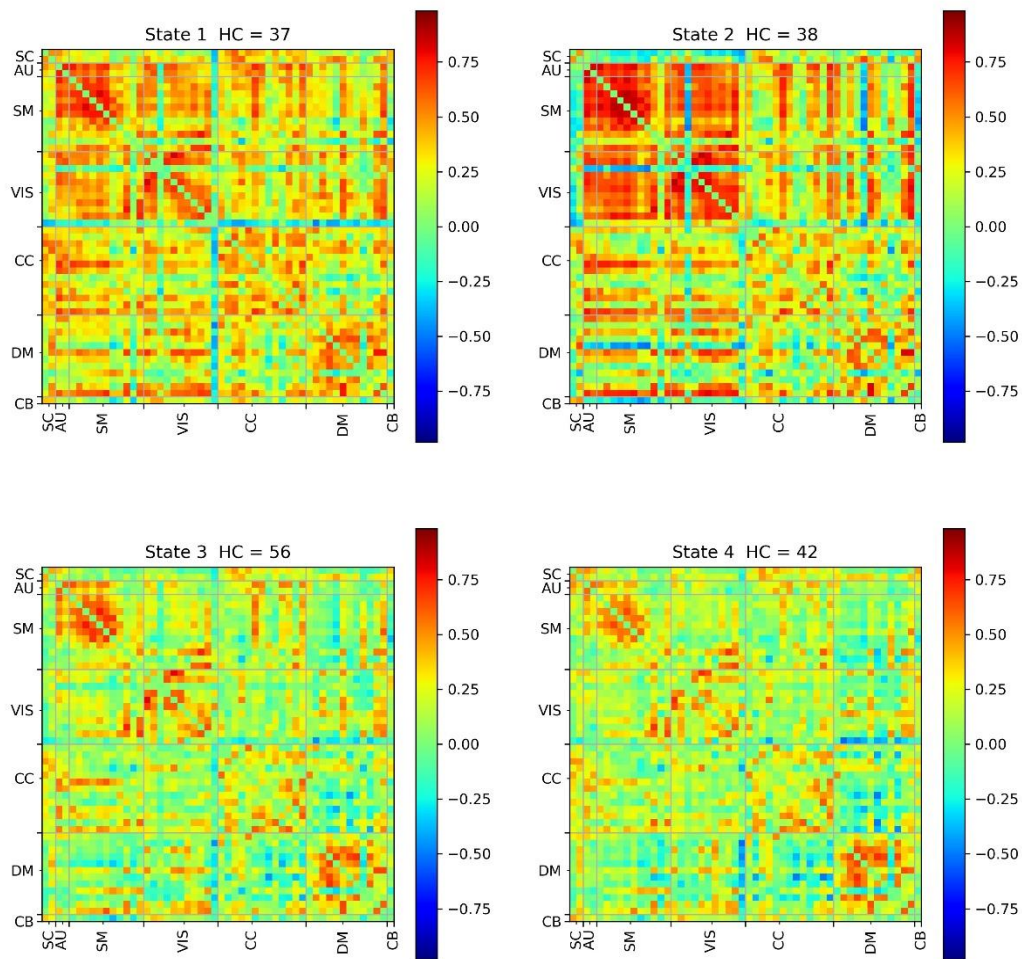


Figure 4.10. Median of correlation matrices in each state for the healthy control subjects.

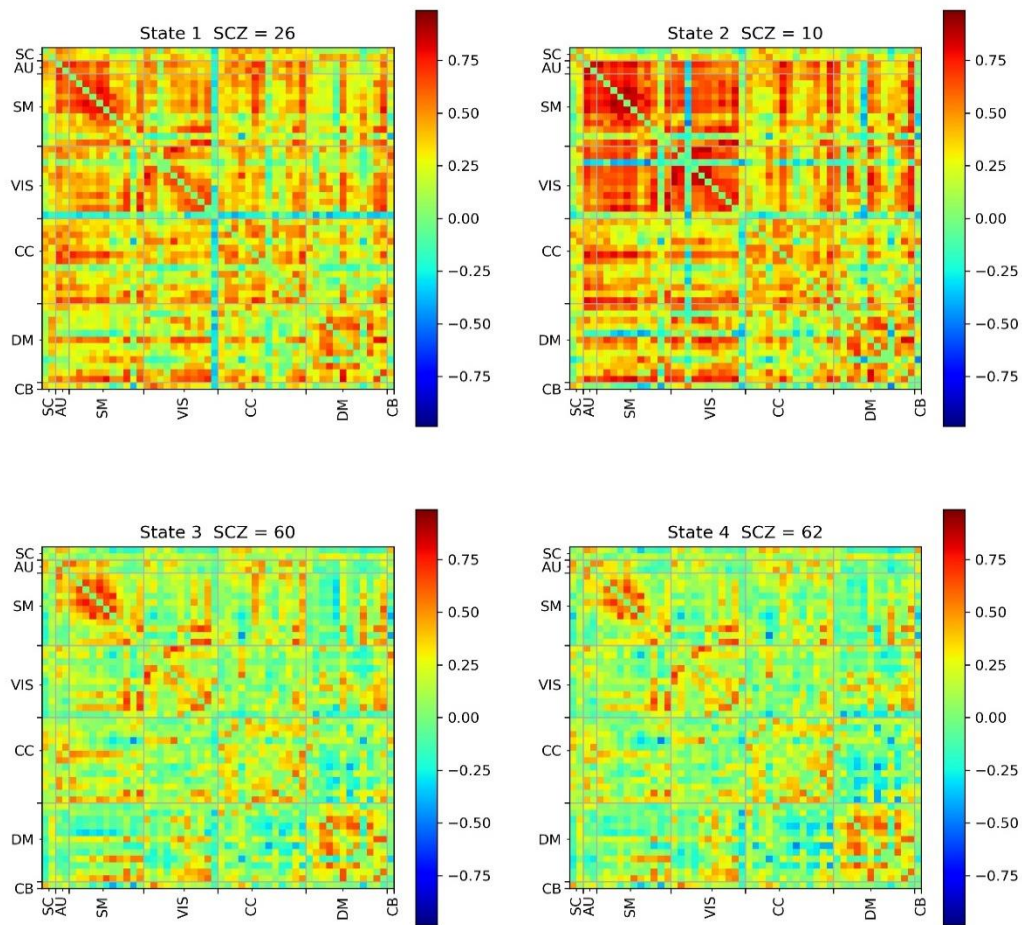


Figure 4.11. Median of correlation matrices in each state for the schizophrenia patients.

4.4 Analysis of Group Differences in Dynamic FC

After clustering all the correlation matrices for obtaining the functional brain connectivity patterns, the group difference between dynamic functional connectivity of the healthy control subjects and that of schizophrenia subjects is studied in this section. For this purpose, a two-sample t -test with

p-value of 0.05 is carried out to detect the group differences for the four identified functional connectivity patterns shown in Figure 4.12. This allows us to determine each pair of the brain regions in the group of the healthy control subjects in which their functional connectivity is significantly different from that in the same pair of brain regions in the group of schizophrenia patients.

By exploring the group-specific median matrices illustrated in Figure 4.10 and Figure 4.11, a moderate to high correlation among the independent components of the VIS, SM and AUD networks are observed in the state 1 and state 2. The moderate and high functional connectivity value between the brain regions (independent components) are demonstrated by the light and dark red color in the correlation matrix. In the states 3 and 4, it is observed that a set of ICs in CC and SM category have antagonism with those in DM. This antagonism is shown by the blue color in the correlation matrix.

From the two-sample t-test results in Figure 4.12, it is shown that there are some brain regions in the healthy control group with the functional connectivity that is significantly different from those in the group of SCZ patients. For example, in Figure 4.12, in the state 2, it can be seen that the functional connectivities between putamen in SC category and some of the components in VIS network in HC group is significantly different from that in the SCZ group. This difference can also be noticed in Figures 4.10 and 4.11 by observing the correlation between the activation signals of SC and VIS in the state 2 of both HC and SCZ groups. It can be seen that there is almost no correlation between the SC and VIS ICNs for the SCZ group while antagonism is observed between these two sets of ICNs for the HC group. Also, it can be seen in the state 3 of Figure 4.12 that the functional connectivity among the components in VIS network of the HC group is different from that of SCZ group. This difference can also be observed from the correlation matrices shown

in Figures 4.10 and 4.11. It can be seen from these figures that there are high correlations among the components in the VIS network for HC group while there is almost no correlation among the same components for the SCZ group. The discussed regions in VIS network in which we have observed difference in the functional connectivity between HC and SCZ groups are also shown on a brain atlas in Figure 4.13.

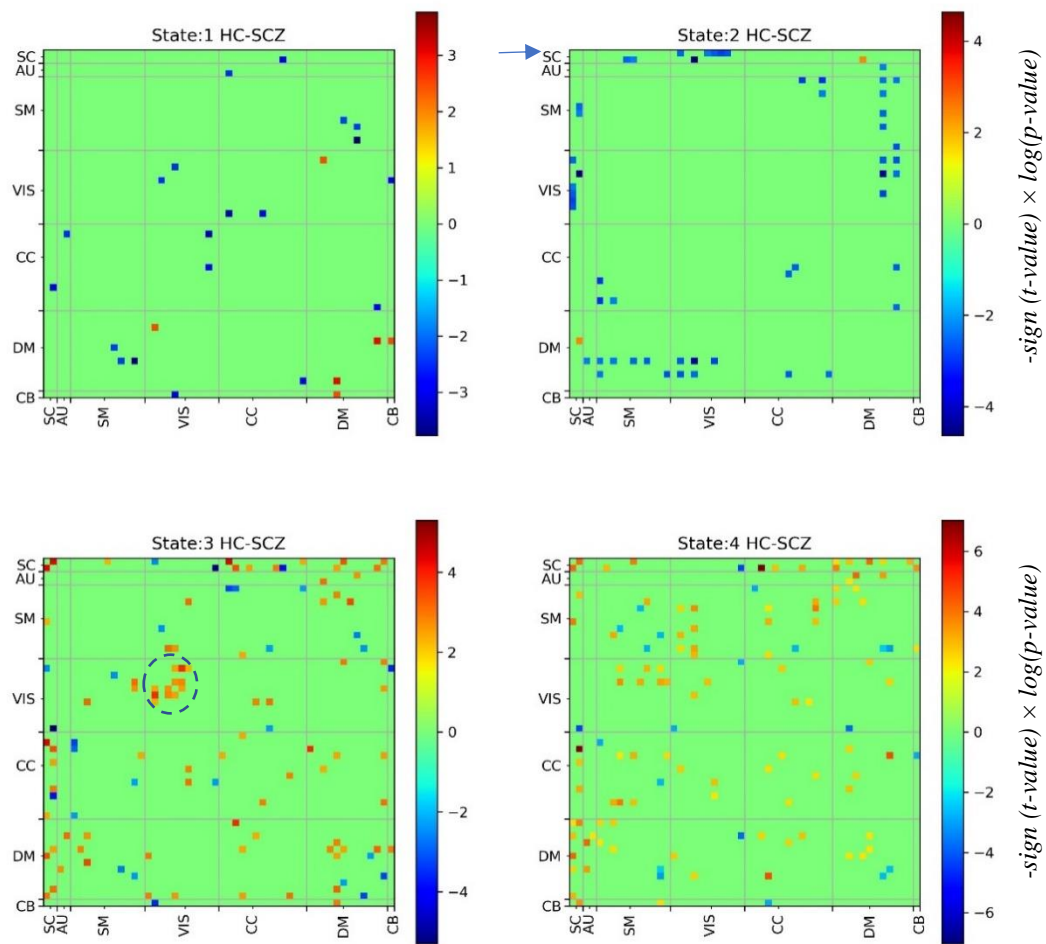


Figure 4.12. Two-sample t-test results showing FC differences between pairs of the brain regions in the healthy control (HC) subjects and corresponding brain regions in the schizophrenia (SCZ) subjects in each state obtained by using the proposed clustering method.

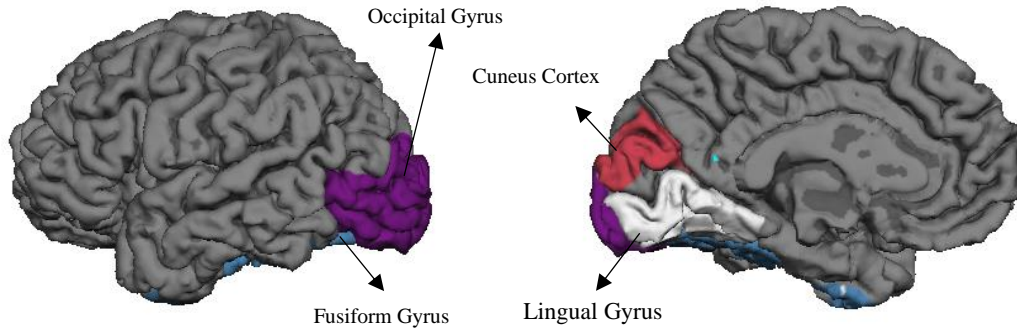


Figure 4.13. Visualization of the regions in the brain visual network where the difference between FCs in the group of HC and those in SCZ is significant by using Freesurfer software.

Also, Figure 4.14 shows the result of two sample t-test when the k-means is applied directly to the connectivity matrices for finding the functional connectivity patterns. Since the performance of the proposed method for clustering the correlation matrices has been shown to be superior to that of k-means clustering, we expect the group difference result shown in Figure 4.12 to be more reliable in compare to that in Figure 4.14.

Dwell time is defined as the time that the functional connectivity remains in one state before switching to another state. In order to show the effectiveness of the proposed method in distinguishing the FC in the healthy people from that in the people affected by schizophrenia, the average dwell times for each group in different connectivity states are computed. Figure 4.15 shows the average dwell time in each state for the HC and SCZ groups after using the proposed method for clustering the connectivity matrices. It can be seen in this figure that the average dwell time for the HC group in the state 2 and state 4 is significantly different from those for SCZ group. In other words, in average, the HC subjects spend significantly more time in the state 2 compared to the SCZ subjects, whereas the patients affected by SCZ spend significantly more time in the state 4 before transition to the other states. Hence, as expected, SCZ subjects remain longer in the

state in which the corresponding average correlation matrix in Figure 4.9 shows the lowest amount of connectivity among brain regions. In contrast, the HC subjects remain longer time in the state in which the corresponding average correlation matrix shows more connectivity between brain region pairs.

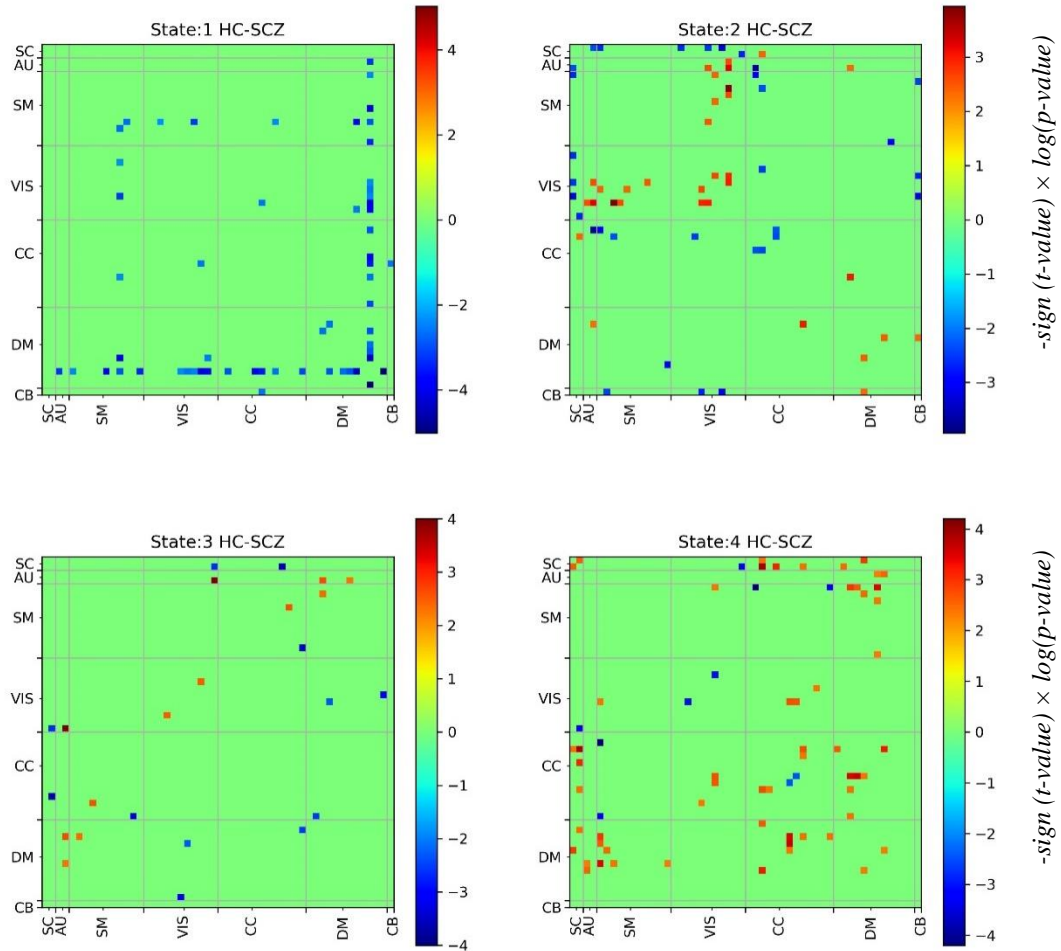


Figure 4.14. Two-sample t-test results showing FC differences between pairs of the brain regions in the healthy control (HC) subjects and corresponding brain regions in the schizophrenia (SCZ) subjects in each state obtained by using the traditional clustering

Also, Figure 4.16 shows the average dwell time in each state for the HC and SCZ groups after clustering the connectivity matrices using the traditional k-means clustering method. It can be seen from this figure that after using the traditional k-means for clustering the connectivity matrices, no significant difference can be observed between the average dwell time of the HC group and that of SCZ group in the state 4. It is against our expectation that SCZ subjects stay longer in the state corresponding to the average correlation matrix showing the less connectivity (state 4 in this case). Hence, it can be concluded that the proposed method for obtaining dynamic functional connectivity provides more meaningful interpretation about the difference in the functional brain connectivity of the HC and that of SCZ subjects.

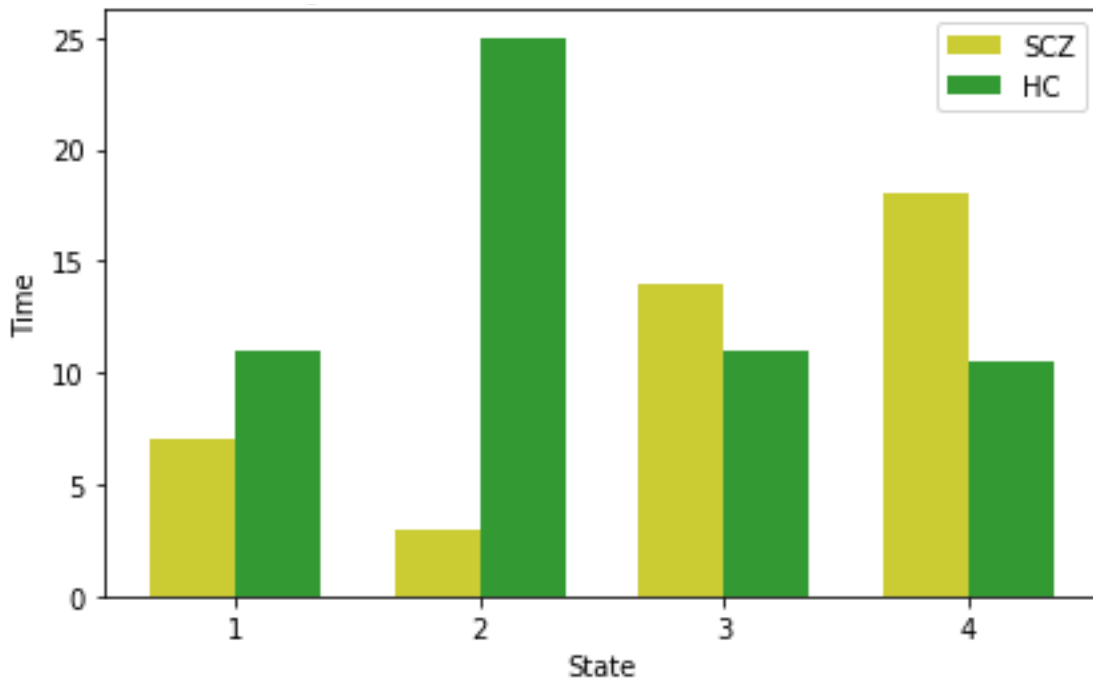


Figure 4.15. Average dwell time in each state for the HC and SCZ groups.

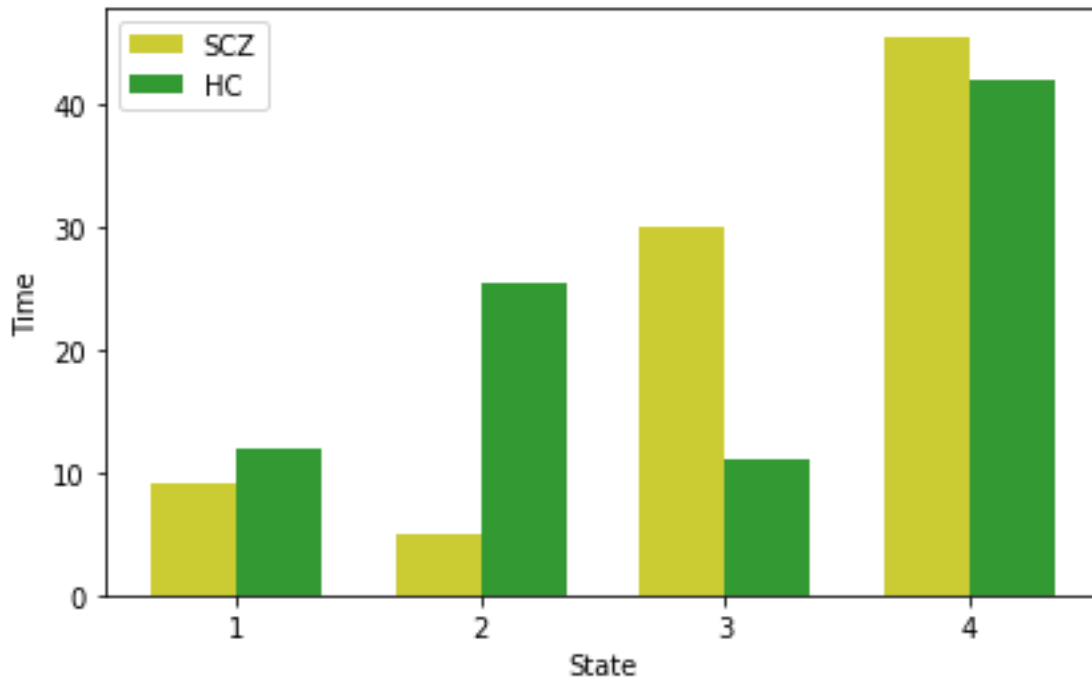


Figure 4.16. Average dwell time in each state for the HC and SCZ groups after applying traditional k-means clustering method.

4.5 Summary

In this chapter, the proposed method for obtaining dynamic functional connectivity using the convolutional autoencoder was evaluated by presenting some experimental results. First, the information about the fMRI data in this study and the parameters used for preprocessing steps were provided. Then, the results for each step of the procedure, including group ICA, component selection, windowing and finding the connectivity matrices were obtained and discussed. The designed convolutional autoencoder was then used for obtaining the latent representations of the correlation matrices. In order to demonstrate the effectiveness of the autoencoder, connectivity matrices with different patterns of known classes are syntactically generated and the performance of the proposed method was compared to that of the k-means applied directly to the connectivity

matrices. The results showed the superiority of the proposed method over k-means. Then, the correlation matrix medians in each state were obtained for both healthy control (HC) and schizophrenia (SCZ) subjects. Finally, a two-sample t -test was performed to detect the group differences between dynamic FC (dFC) of the healthy control (HC) and that of schizophrenia (SCZ) subjects for four the identified connectivity states. We obtained a set of connections in the visual network of HC group with a significant difference to that of SCZ patients. Also, the average dwell time in each state is computed for each group. It was observed that the dwell time for the healthy group to stay in the state with more connectivity was longer than that for the group with schizophrenia. While, the dwell time for the group with schizophrenia to stay in the state with less connectivity is longer than that for the healthy group.

CHAPTER 5: Conclusion and Future Work

5.1 Conclusion

Study of functional connectivity provides a better understanding as to how the brain functions. In the process of studying the dynamic functional connectivity, the independent component analysis (ICA) is performed in order to decompose the functional magnetic resonance imaging (fMRI) data into independent components (map of the entire brain) and their corresponding time-courses. A sliding window is then passed through the time-courses and a correlation matrix is obtained for each segment of the time-courses. In order to obtain the functional connectivity patterns (states), the set of correlation matrices needs to be segmented into cluster of functional connectivity patterns. For this purpose, the k-means for clustering is used. However, it is well-known that the k-means clustering method is not suitable for applying it to high dimensional data such as functional brain connectivity matrices. In this thesis, we have proposed using a deep learning-based convolutional autoencoder to obtain a latent representation of the connectivity matrices prior to applying the k-means clustering. Use of the convolutional autoencoder not only reduces the dimension of the connectivity matrices, but also provides a more semantic representation of these matrices. In order to demonstrate the effectiveness of the autoencoder, connectivity matrices with different patterns of known classes are syntactically generated and the autoencoder is applied to the generated data. The t-distributed stochastic neighbor embedding (t-SNE) is used to visualize the synthetic connectivity matrices and the corresponding latent representations obtained from the convolutional autoencoder. It has been shown through this visualization that the latent representations of the connectivity matrices with the same pattern are close together, whereas they are far apart from those with different patterns. The performance of the proposed method in which

the k-means operation is applied to the latent representations resulting from the convolutional autoencoder has been compared to that of the k-means applied directly to the connectivity matrices. The results have shown the superiority of the proposed method over that of using k-means alone by classifying the various patterns more accurately.

The proposed method has then been used to study the dynamic functional brain connectivity by applying it to real fMRI data captured from 72 healthy subjects and 74 subjects affected by schizophrenia. The group ICA is applied to a preprocessed version of the fMRI data acquired from all the subjects in order to obtain the independent components and their corresponding time-courses. A sliding window is then passed through the time-courses of all the subject to obtain a correlation matrix of the time-courses within each location of the sliding window. Next, the convolutional autoencoder is trained with the connectivity matrices thus obtained. The k-means operation is then applied to the semantic features (latent data) resulting from the convolutional autoencoder to cluster the connectivity matrices into classes of matrices each with a different functional connectivity pattern (state). A two-sample t-test is then performed on each state in order to determine each pair of the regions in the group of the healthy control subjects for which a correlation value is significantly different from that of the corresponding pair of regions in the group of schizophrenia patients. It has been observed from this test that there are indeed pairs of brain regions where such a difference exists between the two groups. It has also been seen that such a difference between the two groups is even more pronounced in the visual network part of the brain.

Finally, in this thesis, a study has been carried out to obtain the average dwell time for the healthy control and schizophrenia subjects in each state. It has been observed that the dwell time for the healthy group to stay in the state with more connectivity is longer than that for the group with

schizophrenia. On the other, the dwell time for the group with schizophrenia to stay in the state with less connectivity is longer than that for the healthy group.

It is expected that the work of this thesis in developing a new scheme for providing a more accurate dynamic connectivity patterns of the brain regions and applying it to determine the differences in the connectivity patterns and in the dwell times between healthy and diseased brain, would help the neurologists and physicians in a more insightful understanding of the brain activities of these groups.

5.2 Future Work

Although the dynamic functional connectivity in resting-state fMRI was studied in this thesis, there are still some limitations that need to be addressed in future. One of the difficulties in this study was to choose the suitable window size for obtaining the correlation matrix within a segment of time-courses enclosed by this window. The length of window must be short enough to capture all the variations in dFC and long enough to get the reliable information of correlation. In future, more research needs to be done for either finding a suitable window size or using variable-sized windows for obtaining functional connectivity matrices. Also, more research for using time-frequency approaches such as wavelet coherence can be carried out to overcome the limitation of window size for study of dynamic functional connectivity.

Finally, it should be noted that the interpretability of results is also an important challenge in the study of dynamic functional connectivity that needs a high level of expertise from neurology experts.

References

- [1] M. G. Preti, T. A. Bolton and D. Van De Ville, “The dynamic functional connectome: state of-the art and perspectives”, *Neuroimage*, vol. 160, pp. 41-54, Oct 2017.
- [2] D. Purves, G. J. Augustine, D. Fitzpatrick, W. C. Hall, A. Lamantia, J. O. Mcnamara, S. M. Williams, “Neuroscience”, 3rd Edition. Sinauer Associates, 2004.
- [3] [Online] available at: <http://buism.com/neurons.htm>.
- [4] [Online] available at: <https://slideplayer.com/slide/7337170/>.
- [5] D. Le Bihan, J.-F. Mangin, C. Poupon, C. A. Clark, S. Pappata, N. Molko, and H. Chabriat, “Diffusion tensor imaging: concepts and applications,” *Journal of magnetic resonance imaging*, vol. 13, no. 4, pp. 534-546, 2001.
- [6] L. Q. Uddin, “Complex relationships between structural and functional brain connectivity”, *Trends in cognitive sciences*, vol. 17, no.12, pp. 600-602, 2013.
- [7] [Online] available at: <http://www.news.ucsb.edu/2013/013501/ucsb-neuroscientists-study-connectivity-human-brain#top>.
- [8] E. A. Allen, E. Damaraju, S. M. Plis, E. B. Erhardt, T. Eichele and V. D. Calhoun. “Tracking whole-brain connectivity dynamics in the resting state.” *Cerebral cortex*, vol. 24, no. 3, pp. 663-676, 2012.
- [9] A. K. Roy, Z. Shehzad, D. S. Margulies, A. C. Kelly, L. Q. Uddin, K. Gotimer, B. B. Biswal, F. X. Castellanos and M. P. Milham, “Functional connectivity of the human amygdala using resting state fMRI,” *Neuroimage*, vol. 45, no. 2, pp. 614-626, 2009.
- [10] C. Chang and G. H. Glover, “Time-frequency dynamics of resting-state brain connectivity measured with fMRI,” *Neuroimage*, vol. 50, no. 1, pp. 81-98, 2010.

- [11] M. De Luca, C. F. Beckmann, N. De Stefano, P. M. Matthews, and S. M. Smith, “fMRI resting state networks define distinct modes of long-distance interactions in the human brain,” *Neuroimage*, vol. 29, no. 4, pp. 1359-1367, 2006.
- [12] S. A. Meda, A. Gill, M. C. Stevens, R. P. Lorenzoni, D. C. Glahn, V. D. Calhoun, J. A. Sweeney, C. A. Tamminga, M. S. Keshavan, G. Thaker and G. D. Pearlson, “Differences in resting-state functional magnetic resonance imaging functional network connectivity between schizophrenia and psychotic bipolar probands and their unaffected first-degree relatives.” *Biological psychiatry*, vol. 71, no. 10, pp.881-889, 2012.
- [13] J. S. Anderson, J. A. Nielsen, A. L. Froehlich, M. B. DuBray, T. J. Druzgal, A. N. Cariello, J. R. Cooperrider, B. A. Zielinski, C. Ravichandran, P. T. Fletcher and A. L. Alexander, “Functional connectivity magnetic resonance imaging classification of autism”, *Brain*, vol. 134, no. 12, pp.3742-3754, 2011.
- [14] M. Greicius, “Resting-state functional connectivity in neuropsychiatric disorders”, *Current opinion in neurology*, vol. 21, no. 4, pp. 424-430, 2008.
- [15] S. A. Huettel, A. W. Song and G. McCarthy, “Functional magnetic resonance imaging”, vol. 1. Sunderland, MA: Sinauer Associates, 2004.
- [16] S. Ogawa, T.M. Lee, A. R. Kay, D. W. Tank, “Brain magnetic resonance imaging with contrast dependent on blood oxygenation”, *Proceedings of the National Academy of Sciences*, vol. 87, no. 24, 1990.
- [17] [Online] available at: <https://www.ndcn.ox.ac.uk/divisions/fmrib/what-is-fmri/introduction-to-fmri>.
- [18] [Online] available at: <http://www.dcs.shef.ac.uk/~haiping/feeler.html>.
- [19] M. E. Raichle, “Two views of brain function”, *Trends in cognitive sciences*, vol. 14, no. 4, pp. 180-190, 2010.

- [20] B. Biswal, F. Zerrin Yetkin, V. M. Haughton and J. S. Hyde, "Functional connectivity in the motor cortex of resting human brain using echo-planar MRI," *Magnetic resonance in medicine*, vol. 34, no. 4, pp. 537-541, 1995.
- [21] C. F. Beckmann, M. DeLuca, J. T. Devlin and S. M. Smith, "Investigations into resting-state connectivity using independent component analysis", *Philosophical Transactions of the Royal Society of London B: Biological Sciences*, vol. 360, no. 1457, pp. 1001-1013, 2005.
- [22] M. P. Van Den Heuvel and H. E. H. Pol, "Exploring the brain network: a review on resting-state fMRI functional connectivity", *European neuropsychopharmacology*, vol. 20, no. 8, pp. 519-534, 2010.
- [23] M. J. Jafri, G. D. Pearlson, M. Stevens and V. D. Calhoun, "A method for functional network connectivity among spatially independent resting-state components in schizophrenia", *Neuroimage*, vol. 39, no. 4, pp.1666-1681, 2008.
- [24] [Online] available at: https://www.researchgate.net/figure/MRI-Scanner-Cutaway-5_fig3_275330507.
- [25] E. Damaraju, E. A. Allen, A. Belger, J. M. Ford, S. McEwen, D. H. Mathalon, B. A. Pearlson, B. A. Mueller, G. D. Pearlson, S. G. Potkin, A. Preda and J. A. Turner, "Dynamic functional connectivity analysis reveals transient states of dysconnectivity in schizophrenia", *NeuroImage: Clinical*, vol. 5, pp. 298-308, 2014.
- [26] R. M. Hutchison, T. Womelsdorf, E. A. Allen, P. A. Bandettini, V. D. Calhoun, M. Corbetta, S. Della Penna, J. H. Duyn, G. H. Glover, J. Gonzalez-Castillo and D. A. Handwerker, "Dynamic functional connectivity: promise, issues, and interpretations", *Neuroimage*, vol. 80, pp. 360-378, Oct 2013.
- [27] R. M. Hutchison, T. Womelsdorf, J. S. Gati, S. Everling, and R. S. Menon, "Resting-state networks show dynamic functional connectivity in awake humans and anesthetized macaques," *Human Brain Mapping*, vol. 34, no. 9, pp. 2154-2177, Sep 2013.

- [28] P. Delamillieure, G. Doucet, B. Mazoyer, M. R. Turbelin, N. Delcroix, E. Mellet, L. Zago, F. Crivello, L. Petit, N. Tzourio-Mazoyer and M. Joliot, “The resting state questionnaire: an introspective questionnaire for evaluation of inner experience during the conscious resting state”, *Brain research bulletin*, vol. 81, no. 6, pp. 565-573, 2010.
- [29] K. Li, L. Guo, J. Nie, G. Li and T. Liu, “Review of methods for functional brain connectivity detection using fMRI”, *Computerized Medical Imaging and Graphics*, vol. 33, no. 2, pp. 131-139, 2009.
- [30] J. Cao, K. J. Worsley, “The geometry of correlation fields, with an application to functional connectivity of the brain”, *The Annals of Applied Probability*, vol. 9, no. 4, pp.1021-1057, 1999.
- [31] M. D. Greicius, B. Krasnow, A. L. Reiss, V. Menon, “Functional connectivity in the resting brain: a network analysis of the default mode hypothesis”, *Proceedings of the National Academy of Sciences*, vol. 100, no. 1, pp. 253-258, 2003.
- [32] M. N. DeSalvo, L. Douw, S. Takaya, H. Liu and S. M. Stufflebeam, “Task-dependent reorganization of functional connectivity networks during visual semantic decision making”, *Brain and behavior*, vol. 64, no. 6, pp.877-885, 2014.
- [33] E. A. Allen, E. B. Erhardt, E. Damaraju, W. Gruner, J. M. Segall, R. F. FSilva, M. Havlicek, S. Rachakonda, J. Fries, R. Kalyanam and A. M. Michael, “A baseline for the multivariate comparison of resting-state networks”, *Frontiers in systems neuroscience*, vol. 5, Feb 2011.
- [34] D. M. Cole, S.M. Smith and C. F. Beckmann, “Advances and pitfalls in the analysis and interpretation of resting-state FMRI data”, *Frontiers in systems neuroscience*, vol. 4, no. 8, 2010.
- [35] E. A. Allen, E. Damaraju, T. Eichele, L. Wu and V. D. Calhoun, “EEG signatures of dynamic functional network connectivity states”, *Brain topography*, vol. 31, no. 1, pp.101-116, 2018.
- [36] J. L. Chen, T. Ros and J. H. Gruzelier, “Dynamic changes of ICA-derived EEG functional connectivity in the resting state”. *Human brain mapping*, vol. 34, no. 1, pp. 852-868, 2013.

- [37] M. Yaesoubi, E. A. Allen, R. L. Miller and V. D. Calhoun, “Dynamic coherence analysis of resting fMRI data to jointly capture state-based phase, frequency, and time-domain information”, *NeuroImage*, vol. 120, pp. 133-142, 2015.
- [38] Z. Yao, B. Hu, Y. Xie, F. Zheng, G. Liu, X. Chen and W. Zheng, “Resting-state time-varying analysis reveals aberrant variations of functional connectivity in autism”, *Frontiers in human neuroscience*, vol. 10, p. 463, 2016.
- [39] Z. Yao, B. Hu, Y. Xie, F. Zheng, G. Liu, X. Chen and W. Zheng, “Resting-state time-varying analysis reveals aberrant variations of functional connectivity in autism”, *Frontiers in human neuroscience*, vol. 10, p. 463, 2016.
- [40] B. Rashid, E. Damaraju, G. D. Pearlson and V. D. Calhoun, “Dynamic connectivity states estimated from resting fMRI Identify differences among Schizophrenia, bipolar disorder, and healthy control subjects”, *Frontiers in human neuroscience*, vol. 8, p.897, Nov 2014.
- [41] X. Guo, X. Liu, E. Zhu, J. Yin, “Deep clustering with convolutional autoencoders”, in *Proc. International Conference on Neural Information Processing*, Springer, pp. 373-382, Nov 2017.
- [42] [Online] available at: <https://www.mccauslandcenter.sc.edu/crnl/tools/stc>.
- [43] [Online] available at: <http://mriquestions.com/data-pre-processing.html>.
- [44] [Online] available at: https://www.slideshare.net/paul_kyeong/introduction-to-neuroimaging.
- [45] [Online] available at: https://www.researchgate.net/figure/Talairach-and-MNI-space_fig10_311612599.
- [46] A. Hyvärinen and E. Oja, “Independent component analysis: algorithms and applications”, *Neural networks*, vol. 13, pp. 411-430, June 2000.
- [47] [Online] available at: <http://www.statsoft.com/Textbook/Independent-Components-Analysis>.

- [48] V. D. Calhoun, T. Adali, G. D. Pearlson and J. J. Pekar. “A method for making group inferences from functional MRI data using independent component analysis”, *Human brain mapping*, vol. 13, no. 3, pp. 140-151, 2001.
- [49] X. Gao, T. Zhang and J. Xiong, “Comparison between spatial and temporal independent component analysis for blind source separation in fMRI data”, in *Proc. IEEE International Conference on Biomedical Engineering and Informatics (BMEI)*, pp. 690-692 October 2011.
- [50] [Online] available at: http://users.ics.aalto.fi/whyj/publications/thesis/thesis_node8.html.
- [51] L. Griffanti, G. Douaud, J. Bijsterbosch, S. Evangelisti, F. Alfaro-Almagro, M. F. Glasser, E. P. Duff, S. Fitzgibbon, R. Westphal, D. Carone and C. F. Beckmann, “Hand classification of fMRI ICA noise components”, *Neuroimage*, vol. 154, pp. 188-205, 2017.
- [52] D. Zhi, V. D. Calhoun, L. Lv, X. Ma, Q. Ke, Z. Fu, Y. Du, Y. Yang, X. Yang, M. Pan and S. Qi, Image in “Aberrant Dynamic Functional Network Connectivity and Graph Properties in Major Depressive Disorder”, *Frontiers in psychiatry*, vol. 9, 2018.
- [53] J. A. Hartigan, M. A. Wong, “Algorithm AS 136: A k-means clustering algorithm” *Journal of the Royal Statistical Society. Applied Statistics, Series C*, pp. 100-108, 1979.
- [54] [Online] available at: “<http://cs231n.github.io/classification/>”.
- [55] [Online] available at: “<https://reexplorations.wordpress.com/2015/08/13/hypothesis-tests-2-sample-tests-ab-tests/>”.
- [56] A. K. Jain, J. Mao and K. M. Mohiuddin, “Artificial neural networks: A tutorial”, *Computer*, vol. 29, no.3, pp.31-44, 1996.
- [57] [Online] available at: “https://en.wikipedia.org/wiki/Artificial_neural_network”.
- [58] [Online] available at: “<https://www.kdnuggets.com/2016/11/quick-introduction-neural-networks.html>”.

- [59] J. Masci, U. Meier, D. Cireşan and J. Schmidhuber, “Stacked convolutional auto-encoders for hierarchical feature extraction”, in *Proc. International Conference on Artificial Neural Networks*, pp. 52-59, Jun 2011.
- [60] [Online] available at: “<https://towardsdatascience.com/build-your-own-convolution-neural-network-in-5-mins-4217c2cf964f>”.
- [61] Y. LeCun and Y. Bengio, “Convolutional networks for images, speech, and time series”, *The handbook of brain theory and neural networks*, MIT Press, M. A. Arbib, Ed. 1995.
- [62] D. Scherer, A. Müller and S. Behnke, “Evaluation of pooling operations in convolutional architectures for object recognition”, *Artificial Neural Networks*, Springer, pp. 92-101, 2010.
- [63] T. J. Churchman, “Reconstructing speech input from convolutional neural network activity”, Unpublished bachelor's thesis, Radboud University Nijmegen, the Netherlands, 2015.
- [64] [Online] available at: “<https://towardsdatascience.com/autoencoders-introduction-and-implementation-3f40483b0a85>”.
- [65] Unknown Author, “Schizophrenia”, *National Institute of Mental Health*, available at: https://www.nimh.nih.gov/health/publications/schizophrenia/nih_15-3517_155600.pdf.
- [66] [Online] available at: http://fcon_1000.projects.nitrc.org/indi/retro/cobre.html.
- [67] [Online] available at: <https://www.fil.ion.ucl.ac.uk/spm/software/spm12/>.
- [68] [Online] available at: <http://mialab.mrn.org/software/gift/>.
- [69] J. Himberg, A. Hyvarinen, “Icasso: software for investigating the reliability of ICA estimates by clustering and visualization”, in *Proc. IEEE Neural Networks for Signal Processing workshop*, pp. 259-268, 2003.
- [70] [Online] available at: <https://www.nitrc.org/projects/mricron>.

- [71] Z. Ghahramani and M. J. Beal, “Variational inference for Bayesian mixtures of factor analysers”, *Proceedings of Advances in Neural Information Processing Systems*, vol. 12, pp. 449–455, 2000.